Fluvial Ge/Si Ratios in the Copper River Basin, Alaska: Implications for the Global Germanium and Silicon Cycles

Alison M. Anders

A thesis submitted in partial fulfillment of the requirements for the degree of
Master of Science

University of Washington
2001

Program Authorized to Offer Degree: Department of Earth and Space Sciences

TABLE OF CONTENTS

LIST OF FIGURES

LIST OF TABLES

Introduction

The Quaternary is characterized by periodic switches between glacial and interglacial climates that can be detected in numerous geomorphic, sedimentalogic, biologic, and chemical paleoclimate records from around the globe. These climate changes were first recognized through terrestrial evidence of the growth and decay of ice sheets in the mid-latitudes. More recently, evidence that changes in the chemistry of the atmosphere and oceans occurred along with changes in global ice volume has forced the study of Quaternary climate change to include the complex relationships between the ocean, atmosphere, land surface and global climate.

The Vostok ice core revealed that atmospheric carbon dioxide (CO_2) partial pressures have varied from glacial lows of 200 μatm to interglacial values of 280 μatm. These pCO_2 variations show a tight correlation with temperature and ice volume proxy records for the last four glacial cycles (Petit et al., 1999). The ratio of the trace element germanium to silicon in the ocean as recorded in opal from marine cores also show significant changes that have occurred in phase with changes in global ice volume and atmospheric CO_2 levels (Figure 1). The causes and consequences of the low atmospheric CO_2 levels during glacial periods and high atmospheric CO_2 levels during interglacials remain as significant outstanding issues in the earth sciences more than 15 years after their discovery (Archer et al., 2000). In addition, the understanding of the impact of climate changes on germanium and silicon cycles remains in its infancy.

Terrestrial chemical weathering of silicate minerals provides a link between atmospheric carbon dioxide levels and oceanic germanium to silicon (Ge/Si) ratios. Atmospheric CO_2 is closely tied to chemical weathering because the weathering of silicate minerals creates the alkalinity and calcium ions that eventually lead to precipitation of carbonate minerals in the ocean. This process effectively remove CO_2 from the atmosphere and stores it until the carbon is released during volcanic events or chemically weathered (Ruddiman et al., 1997). Controls on the rate of silicate weathering reactions are, therefore, controls on the rate of removal of CO_2 from the atmosphere by chemical weathering. Over the 10^3-10^4 year timescale, this can significantly impact the concentration of CO_2 in the atmosphere (Kump and Alley, 1994; Ruddiman et al., 1997). Chemical weathering of silicate minerals is also the main source of silicon and germanium to the ocean (Froelich et al., 1985; Treguer et al., 1995). The ratio of germanium to silicon in the dissolved load of rivers has been suggested to be controlled by the chemical weathering intensity, defined as the fraction of bedrock silicon that

is removed in solution (Murname and Stallard, 1990). Furthermore, changes in weathering intensity on the continents are the dominant explanation for the glacial to interglacial variations in oceanic Ge/Si ratio (Froelich et al., 1992; Munhoven and Francois, 1996).

The impact of glaciation on germanium and silicon cycles is not well understood. If the relationship between Ge/Si and weathering intensity in glacial environments can be deciphered, this will allow for better interpretation of the oceanic Ge/Si record and the role of glacial-interglacial changes in atmospheric pCO_2. This study compares the Ge/Si ratios between adjacent glacial and periglacial environments to isolate the effect of current glacial activity from the impacts of climate, topography and past glaciation. The glacial and periglacial basins are also compared to other world rivers to examine how these high-latitude, physically-erosive environments differ from warmer and more stable environments.

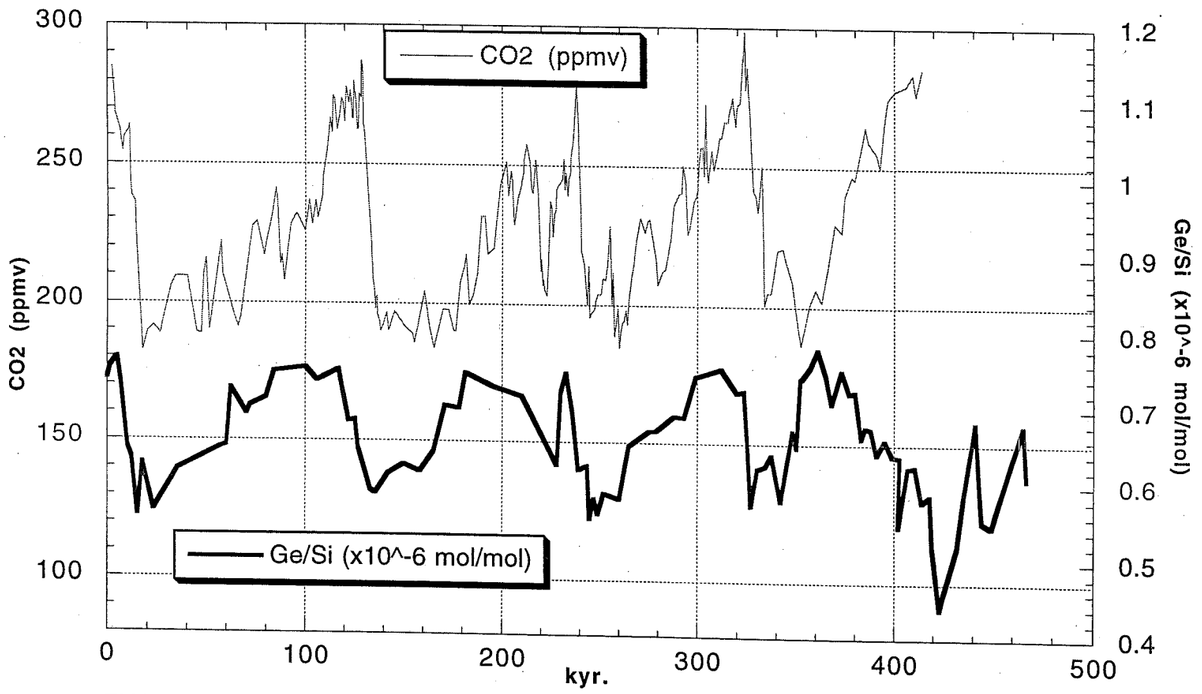

FIGURE 1: Ocean Ge/Si and Atmospheric CO_2 Variations During the Last 450,000 Years
The Ge/Si of opal cores from the South Atlantic (Froelich et al., 1992) are remarkably well correlated with atmospheric CO_2 levels as recorded in the Vostok ice core (Petit et al., 1999). Silicate weathering may provide a link between these records

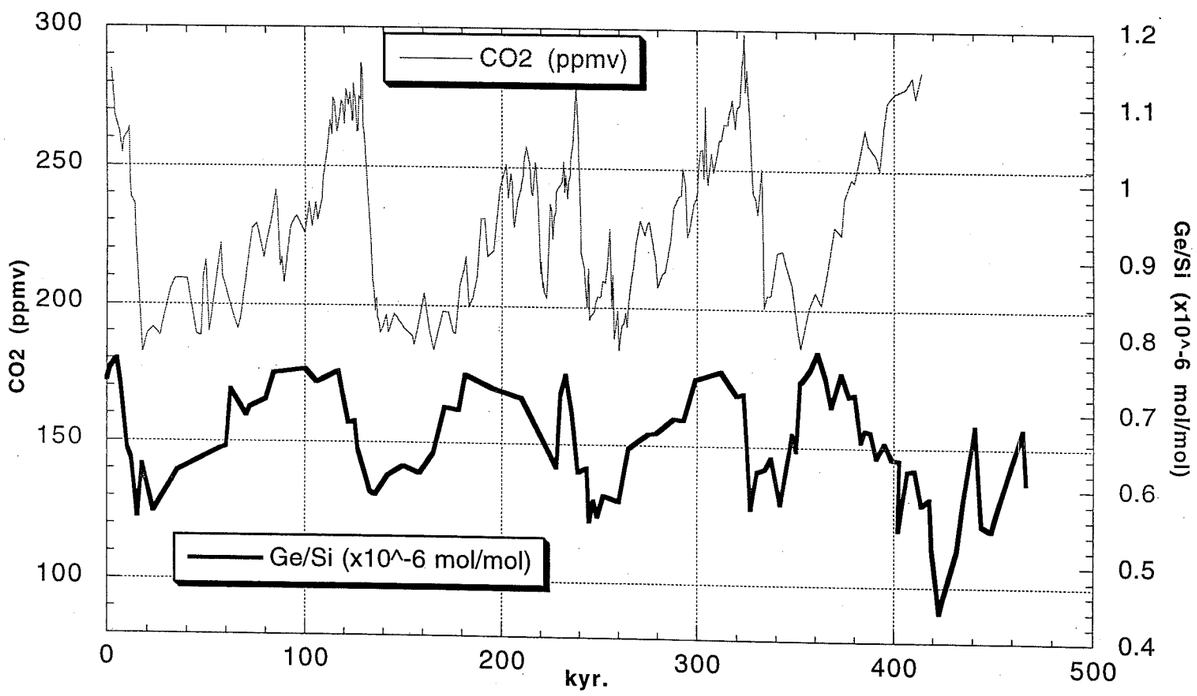

FIGURE 1: Ocean Ge/Si and Atmospheric CO_2 Variations During the Last 450,000 Years
The Ge/Si of opal cores from the South Atlantic (Froelich et al., 1992) are remarkably well correlated with atmospheric CO_2 levels as recorded in the Vostok ice core (Petit et al., 1999). Silicate weathering may provide a link between these records

Background

Germanium and Silicon Cycles

Germanium is a trace element with very similar geochemical behavior to silicon, acting much like a heavy isotope of silicon (Burton et al., 1959; Bernstein, 1985; Froelich et al., 1992). Germanium and silicon have similar ionic radii, ionization potential, and outer electron configuration (Burton et al., 1959). Germanium is strongly quadrivalent and usually occurs in tetrahedral coordination with oxygen, much like silica (Bernstein, 1985). In laboratory experiments, minerals with structures analogous to those of the silicates have been made with germanium replacing the silicon (Bernstein, 1985). In addition, germanium is found to substitute for silicon in the lattices of naturally occurring silicate minerals (Burton et al., 1959; Bernstein, 1985).

Germanium is enriched in chain and layer silicates over more cross-linked structures, resulting in about 50% more germanium occurring in pyroxenes, olivines and amphiboles compared to feldspars (Burton et al., 1959; Bernstein, 1985). It is also enriched in low-temperature, late-forming phases in magmatic systems such as pegmatites and skarns (Burton et al., 1959). Despite these differences, the average germanium concentrations in mafic and felsic igneous rocks are nearly indistinguishable at about 1.5 ppm (Table 1). The germanium concentration of carbonates, sulfates, and evaporites is very low (less that about 0.09 ppm). Germanium can be greatly enriched in iron oxide and sulfide ores, which are the source for commercial germanium (Bernstein, 1985). In these ores, germanium is associated with zinc, copper and lead (Bernstein, 1985). Germanium is also enriched in topaz, fluorite and micas, suggesting a germanium fluoride species may form (Bernstein, 1985). A sulfur-germanium species is likely, given the association with sulfide minerals (Bernstein, 1985). Coal is also known to be enriched in germanium and coal burning has dramatically increased the Ge/Si ratio of many mid-latitude rivers (Froelich et al., 1992).

The ocean contains germanium at a concentration of about 1.7 ppt and the residence time is 10-20,000 years (Froelich and Andreae, 1981; Froelich et al., 1985). In the ocean, germanium is cycled like silicon and taken up in the shells of siliceous organisms without significant fractionation (Froelich et al., 1992; Bareille et al., 1998). Germanium and silicon, therefore, have a near spatially uniform ratio in today's ocean of 0.735 pmol/μmol (Froelich and Andreae, 1981). In addition, the record of Ge/Si changes in biogenic opal over glacial to

interglacial time is likely to represent whole-ocean changes (Froelich et al., 1992). To explore the possible mechanisms of change, a more detailed understanding of the sources and sinks of germanium in the oceans is necessary.

Dissolved germanium is supplied to the ocean via fluvial and groundwater transport, hydrothermal vents on the seafloor, and dissolution of wind-blown dust in the ocean (Figure 2). These different supplies of germanium have distinct Ge/Si signatures (Froelich et al., 1992). The average river value of Ge/Si is 0.54 pmol/μmol and rivers supply an estimated 70% of germanium to the ocean (Froelich et al., 1992). Hydrothermal vents supply germanium at a Ge/Si ratio of about 7 pmol/μmol (Froelich et al., 1992). Groundwater and dust fluxes to the ocean are more difficult to quantify, both in terms of Ge/Si ratio and absolute mass transport. Aeolian material is expected to be enriched in Ge/Si relative to continental crust because of the observed increase in Ge/Si in soils (Munhoven and Francois, 1996). However, during glacial periods, the source of dust may shift from soils to primary mineral fragments derived from glacial grinding. Kurtz (1998) found that dust-derived pelagic sediments are enriched in Ge/Si and depleted in Si/Al relative to loess – indicating that once the dust reached the ocean, some of the silicon and germanium was dissolved to contribute a low Ge/Si flux to the ocean. In addition to the sink of germanium in siliceous-shelled animals, another sink of germanium is necessary to balance the germanium budget as it is currently quantified (Zhou and Kyte, 1991; Elderfield and Schultz, 1996). King et al. (2000) have observed early diagenesis of germanium, uncoupled from opal, in near-anoxic sediments in the South Atlantic and suggest this mechanism may remove germanium from the ocean.

Changes in the flux or ratio of germanium and silica through any part of the germanium cycle may be responsible for the observed changes in the oceanic Ge/Si through glacial cycles. However, given the associations between chemical weathering of silicates and atmospheric carbon dioxide levels, and, the likelihood of changes in weathering on the continents with climate, I have chosen to examine more closely the control on the fluvial Ge/Si ratio in glacial and periglacial settings as compared to non-glacial settings.

In river waters, germanium occurs at levels of about 0.5 to 10 ppt and the Ge/Si ratio is nearly always lower than that of the drainage basin bedrock (Froelich et al., 1992). The world average river Ge/Si ratio is 0.6 pmol/μmol while the continental crust Ge/Si ratio is about 1.5 pmol/μmol (Froelich et al., 1992). The low fluvial ratio implies that there is a process partitioning germanium and silicon during rock weathering (Murname and Stallard, 1990). Germanium is enriched in secondary clay minerals, suggesting that preferential retention of

germanium during weathering is a mechanism for depleting germanium relative to silicon in river water (Murname and Stallard, 1990). A schematic model of this partitioning is presented in Figure 3. However, a detailed study of the possible mechanisms and rates of this partitioning has not been undertaken.

The Ge/Si of rivers has been associated with the stability of the land surface they drain. This association led Murname and Stallard (1990) to develop a model of the controls of germanium and silicon in rivers. They defined chemical weathering intensity as the fraction of bedrock silicon that is ultimately removed from a basin in the dissolved load rather than the bedload or suspended load. Weathering intensity is correlated with the erosional regime as can be illustrated by two end-member cases. In a low chemical weathering intensity environment, most of the silicon is removed from the basin as suspended or bedload (Murname and Stallard, 1990). The transport of relatively unaltered suspended sediment is correlated with steep topography, thin soils, and rapid physical erosion (Murname and Stallard, 1990). The Ge/Si ratio of rivers in a low weathering intensity environment is low because of the dominance of primary mineral weathering. The limiting case of the opposite end-member, a high-weathering intensity regime, would allow all the Si in the bedrock to be transported as dissolved material (Murname and Stallard, 1990). Vanishing relief, thick soil, warm climates and very slow physical erosion are required for the weathering intensity to be high (Murname and Stallard, 1990). In high weathering intensity basins, dissolution of clay minerals can contribute significantly to the solute load, creating a high Ge/Si ratio in the rivers.

Perhaps counterintuitively, the concentration of dissolved Si in rivers is inversely related to weathering intensity, and Ge/Si (Figure 4). The concentration of dissolved Si in a river draining a low-weathering intensity region is likely to be higher than that of a river draining a high weathering intensity region where weathering reactions have stripped off the easily soluble ions and weathering proceeds very slowly (Murname and Stallard, 1990). In fact, in high weathering intensity regions, Si may be the largest component of the relatively small dissolved load (Murname and Stallard, 1990).

The depletion of the trace element Ge with respect to Si during weathering can be used to estimate weathering intensity (Murname and Stallard, 1990). Assuming there is no storage of Ge or Si in groundwater and a negligible effect of bedload, the Ge/Si ratio of the bedrock, suspended load and dissolved load must be simply related to the weathering intensity (I) via the following equation (Murname and Stallard, 1990):

$$\left(\frac{Ge}{Si}\right)_{bedrock} = I*\left(\frac{Ge}{Si}\right)_{dissolved} + (1-I)*\left(\frac{Ge}{Si}\right)_{suspended}$$

If we assume a simple linear relationship between the Ge/Si ratio of the suspended load and the weathering intensity and that the suspended load ratio equals the bedrock ratio when the intensity is zero, an empirical partitioning coefficient (A) can be defined such that:

$$\left(\frac{Ge}{Si}\right)_{Suspended} = \left(\frac{Ge}{Si}\right)_{bedrock} + A \cdot I \quad \text{and} \quad \left(\frac{Ge}{Si}\right)_{dissolved} = \left(\frac{Ge}{Si}\right)_{bedrock} + A \cdot (I-1)$$

The weathering intensity as well as A can be estimated by finding the Ge/Si ratio in the bedrock, dissolved load and suspended load under several different weathering intensity regimes in a region (Murname and Stallard, 1990). The average world weathering intensity is estimated to be 0.12 (Murname and Stallard, 1990). Typical values for A range from 2.5 to 3 (Froelich et al., 1992).

The influence of glaciation on the Ge/Si of rivers is not well known and few data exist. Chillrud et al. (1994) measured the Ge/Si in three glacial streams in the Argentine Andes and found comparatively high values of 0.65 to 1.4 pmol/μmol, including the highest values in the catchment. In contrast, changes in the global climate during glacial periods, both in ice-covered and ice-free regions, are suggested to have decreased overall chemical weathering intensity on the continents (Froelich et al., 1992). These findings prompted Munhoven and Francois (1996) to create a model of the carbon cycle and the germanium and silicon cycles over glacial-interglacial time periods. Atmospheric CO_2 and Ge/Si records can be successfully simulated by forcing the world fluvial flux of silicon to be 2-3 times the present and the Ge/Si ratio to be lower (Munhoven and Francois, 1996). This scenario is unappealing, however, because it is generally accepted that the climate was drier during glacials, so fluvial discharge is unlikely to be increased during glacials. While the flux of silica need not scale with the discharge, a large increase in the concentration of germanium and silica in rivers also seems unlikely. The questionable success of this model and the apparent contradiction between the high Ge/Si ratios in the few glacial rivers for which data exist (Chillrud et al., 1994) and the general condition of low weathering intensity in glacial environments provides interesting motivation for studying the direct influence of glaciation on Ge/Si ratios. To begin to address this issue, a careful consideration of the nature of chemical weathering in glacial environments is necessary.

Subglacial Chemical Weathering

Physical erosion by glaciers can be much more rapid than erosion in the absence of glacial ice. Hallet et al. (1996) showed that glacial physical erosion rates are often orders of magnitude higher than non-glacial rates. In light of the significance of physical erosion in glacial settings and the connections between physical and chemical erosion, it is natural to investigate chemical erosion in glacial systems.

It has long been known that chemical weathering occurs subglacially, especially in alpine glacial settings (Reynolds and Johnson, 1972). In fact, cation denudation rates in small alpine glacial basins are usually 1.2 to 4 times the world average (Souchez and Lemmens, 1987) although these rates are not higher than those for non-glaciated basins with similar specific discharge (Anderson et al., 1997). Alaska and Iceland show chemical weathering rates up to 35 times the world average (Sharp et al., 1995). These rates observed in temperate glacial environments cannot be extrapolated to large ice sheets, however, because it is likely that ice sheets are largely frozen to their beds and that the supply of atmospheric carbon dioxide to the bed is small (Gibbs and Kump, 1994; Kump and Alley, 1994; Hallet et al., 1996).

High cation denudation rates from glacial catchments probably arise from the presence of large amounts of fine and mechanically weakened sediment. In laboratory experiments, glacial flour has been shown to be chemically very reactive (Tranter et al., 1993; Collins, 1995; Brown et al., 1996; Anderson et al., 2000), likely due to the large area of unweathered surfaces. Indeed, the weathering rate is inversely proportional to the grain size in lab experiments on glacial sediment from the Haut Glacier d'Arrola in the Swiss Alps by Brown et al. (1996). In addition, they suggested that subglacial abrasion and crushing of sediment can weaken the crystal lattice and modify the surface to be more reactive.

Another factor that contributes to the solute acquisition by glacial meltwater is the mixing of sediment-rich subglacial water with dilute, carbon-dioxide carrying supra- and englacial meltwater (Raiswell and Thomas, 1984; Tranter et al., 1993; Brown et al., 1994; Chillrud et al., 1994; Brown et al., 1996). The mixing of these waters, either in subglacial channels or near the glacier terminus, results in the rapid release of cations from the suspended sediment and an increase in pH (Tranter et al., 1993; Brown et al., 1996). Therefore, glacial flour may weather subglacially or while in transit in the glacio-fluvial system. In addition, glacial sediment continues to be highly reactive after deposition. Anderson et al. (2000) found that at the Bench Glacier in Southeast Alaska, solute fluxes from young glacial sediments were 3-4

Subglacial Chemical Weathering

Physical erosion by glaciers can be much more rapid than erosion in the absence of glacial ice. Hallet et al. (1996) showed that glacial physical erosion rates are often orders of magnitude higher than non-glacial rates. In light of the significance of physical erosion in glacial settings and the connections between physical and chemical erosion, it is natural to investigate chemical erosion in glacial systems.

It has long been known that chemical weathering occurs subglacially, especially in alpine glacial settings (Reynolds and Johnson, 1972). In fact, cation denudation rates in small alpine glacial basins are usually 1.2 to 4 times the world average (Souchez and Lemmens, 1987) although these rates are not higher than those for non-glaciated basins with similar specific discharge (Anderson et al., 1997). Alaska and Iceland show chemical weathering rates up to 35 times the world average (Sharp et al., 1995). These rates observed in temperate glacial environments cannot be extrapolated to large ice sheets, however, because it is likely that ice sheets are largely frozen to their beds and that the supply of atmospheric carbon dioxide to the bed is small (Gibbs and Kump, 1994; Kump and Alley, 1994; Hallet et al., 1996).

High cation denudation rates from glacial catchments probably arise from the presence of large amounts of fine and mechanically weakened sediment. In laboratory experiments, glacial flour has been shown to be chemically very reactive (Tranter et al., 1993; Collins, 1995; Brown et al., 1996; Anderson et al., 2000), likely due to the large area of unweathered surfaces. Indeed, the weathering rate is inversely proportional to the grain size in lab experiments on glacial sediment from the Haut Glacier d'Arrola in the Swiss Alps by Brown et al. (1996). In addition, they suggested that subglacial abrasion and crushing of sediment can weaken the crystal lattice and modify the surface to be more reactive.

Another factor that contributes to the solute acquisition by glacial meltwater is the mixing of sediment-rich subglacial water with dilute, carbon-dioxide carrying supra- and englacial meltwater (Raiswell and Thomas, 1984; Tranter et al., 1993; Brown et al., 1994; Chillrud et al., 1994; Brown et al., 1996). The mixing of these waters, either in subglacial channels or near the glacier terminus, results in the rapid release of cations from the suspended sediment and an increase in pH (Tranter et al., 1993; Brown et al., 1996). Therefore, glacial flour may weather subglacially or while in transit in the glacio-fluvial system. In addition, glacial sediment continues to be highly reactive after deposition. Anderson et al. (2000) found that at the Bench Glacier in Southeast Alaska, solute fluxes from young glacial sediments were 3-4

times higher than the from discharge of the glacier system itself. Moreover, the silicate reaction rates of glacial sediment are much higher once vegetation is established (Anderson et al., 2000).

The contribution of trace constituents to the chemical character of glacial waters is very high relative to that in subaerial rivers. The dominant chemical weathering under mountain glaciers is often reported to be calcite dissolution and pyrite oxidation with subsequent attack by sulfuric acid produced during sulfide oxidation (Drever and Hurcomb, 1986; Tranter et al., 1993; Brown et al., 1994; Sharp et al., 1995; Fairchild et al., 1999; Anderson et al., 2000). Biotite weathering to vermiculite is found to account for the bulk of silicate weathering subglacially and glacial discharge is also often characterized by high potassium concentrations and high $^{87}Sr/^{86}Sr$ ratios (Blum et al., 1994; Blum and Erel, 1995; Anderson et al., 1997; Anderson et al., 2000). Weathering of calcite and pyrite and weathering by sulfuric acids do not lead to the long-term removal of carbon dioxide from the atmosphere. This finding led Anderson (1997), and Harbor and Warburton (1993) to conclude that the carbon dioxide consumption is not more rapid in glacial environments than in non-glacial environments. Carbon dioxide drawdown in both glacial and non-glacial catchments, however, does scale with discharge (Sharp et al., 1995; Anderson et al., 1997)

Gauging the net impact of glaciation on silicate weathering would require an understanding of the changes in runoff, land area, the exposure area of various rock types, and the extent of reworking of proglacial sediments. In spite of the dearth of information about these changes, a number of connections between glaciation and both global germanium and silicon cycles can be anticipated. Glacial systems are regions of low intensity chemical weathering: despite the reactivity of sediment, mechanical erosion dominates and the overwhelming bulk of silicon is removed from the basin by wind or water as solid material. It is difficult to anticipate the effect of weathering of fine glacial sediment, in either subglacial or periglacial environments, on the Ge/Si ratios of rivers in cold regions because silicate weathering is much slower in dilute, cold waters relative to warmer regions, where soils form relatively rapidly, that Murname and Stallard (1990) considered in their model of fluvial Ge/Si ratios. Secondary minerals do not often accumulate in subglacial environments since the material is transported so rapidly that removal of material is not sufficient to change the bulk composition of a grain – they remain largely unaltered. It is unclear how the mechanisms that partition germanium and silicon in soil-forming environments might operate in subglacial environments. A field study of the germanium and silicon ratios in glacial and periglacial environments in the Copper River Basin of south-central Alaska was undertaken to address these issues.

Table 1: Germanium Concentrations and Ge/Si in Selected Terrestrial Materials

References as follows: 1:(Burton et al., 1959), 2:(Bernstein, 1985) 3:(Bernstien and Waychunas, 1987) 4:(Froelich et al., 1992) 5:(Filippelli et al., 2000)

Material	Ge (ppm)	Ref.	Ge/Si (pmol/μmol)	Ref.
Average Continental Crust	1.5	1	1.4	4
Basalts	0.7 – 3.1	2	2.6 ± 0.2	4
Granite	0.5 – 4.0	2	1.29	5
Biotite	1.2 – 8.5	1	4.10	5
Muscovite	1.1 – 6.5	2	2.00	5
Average Clays	1.4 – 2.8	2	3.5	4
Carbonate Sediments	0.02 -0.09	1		
Pyrite	0.4 – 0.7	2		
Iron Hydroxide Precipitates	11-100	3		

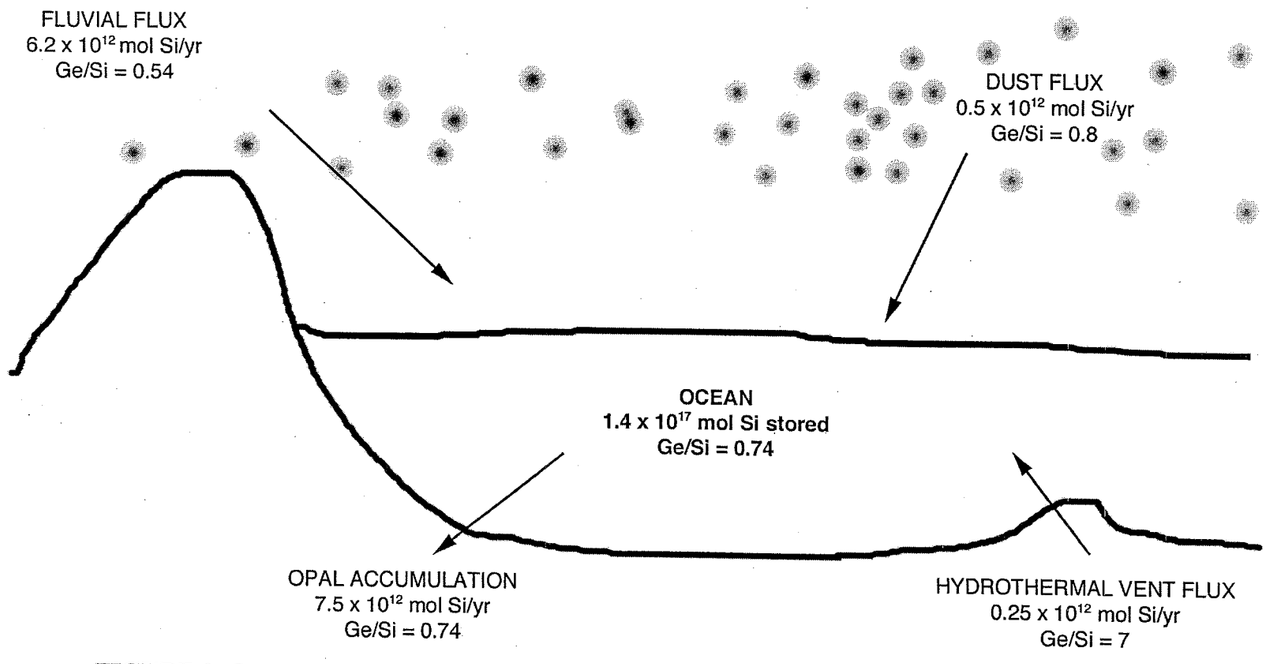

FIGURE 2: Ocean Budget of Silicon and Germanium
The best estimates of fluxes and Ge/Si ratios of the major Ge and Si sources and sinks to the ocean. Fluvial and dust fluxes and opal accumulation are from Treguer et al., (1995). Hydrothermal vent flux is from Mortlock et al. (1993). The ocean reservor size is from Broecker and Peng (1982). All Ge/Si ratios except that for dust are from Froelich et al. (1992). The Ge/Si ratio of dust is not well constrained - aeolian material is estimated to have a Ge/Si ratio of 0.9-2.6 (Mortlock and Froelich, 1987). However, Kurtz (1998) found evidence for incongruent weathering of dust in the ocean - making the Ge/Si ratio of the dust contribution lower than that of the ocean.

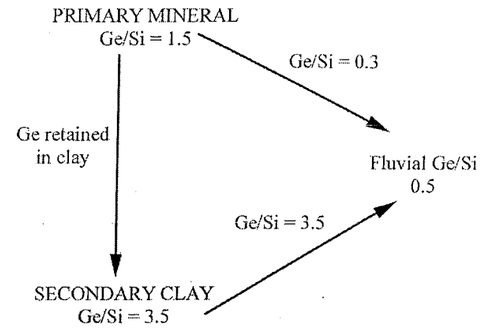

FIGURE 3: Incongruent Weathering and Fluvial Ge/Si
Murname and Stallard's (1990) model of fluvial Ge/Si ratios includes includes inputs from two sources. Primary mineral weathering is incongruent: Ge is retained in clay minerals with an average world fractionation factor of 2.5. The initial solutes from primary mineral weathering have a very low Ge/Si ratio of 0.3. The dissolution of secondary clay minerals has a Ge/Si ratio that is higher than the initial bedrock and approaches that of the clay mineral - about 3.5. Primary and secondary mineral weathering represent low and high weathering intensity, respectively.

FIGURE 4: Ge/So Mixing Line for Clean Rivers
Clean world rivers plot along a mixing line between a high Si, low Ge/Si, low weathering intensity end member and a low Si, high Ge/Si, high weathering intensity end member. Figure 4 is modified from Froelich et al. (1992).

Sample Collection and Analysis

The Copper River basin of south-central Alaska was chosen as the field area because it allows for easy sampling of glacial and periglacial rivers in four different regions with distinct topography and lithology: the Wrangell Mountains, Alaska Range, Chugach mountains and the Copper Basin interior (Figure 5).

The Wrangell Mountains are in the Wrangellia Terrane and the dominant lithologies in this area include basalts locally metamorphosed to lower greenschist facies, limestone, sandstone, marine clastics and volcaniclastics, and minor granitic and metagranite plutons (Nokleberg et al., 1994). The eastern end of the Alaska Range is partially within the Wrangellia Terrane and contains many of the same formations. The central Alaska Range, in the Gulkana River area is dominantly composed of three metamorphic sequences including chlorite and pelitic schist, calcite and dolomite marble, schistose diorite and schistose granite. The Chugach Mountains are also partially within the Wrangellia Terrane and more of the deeper levels are exposed including the basement metagranite and metadiorite (Nokleberg et al., 1994). In addition, the Chugach Mountains include the Peninsular Terrane that comprises a metamorphic mafic-ultramafic basement, limestones, basalts and andesites, the granitic Alaska-Aleutian Range Batholith, and a marine calcareous and volcanic sequence (Nokleberg et al., 1994). The interior of the Copper River basin is underlain by the Wrangellia and Peninsular Terranes. However, a thick sequence of fluvial, glacial and lacustrine deposits and andesitic lavas fills this central basin (Nokleberg et al., 1994).

Samples were taken from 50 sites within the Copper River Basin including five sites along the main stem of the Copper River, and along glacial and periglacial tributaries of the Copper River (Figure 5). At each site, a description of the flow conditions, channel width, and bank material was recorded. A handheld GPS unit was used to establish the location of the site. A Millipore filtration system was used to filter water. The filter system funnel and flask and the collection bottle were rinsed three times in the river. 200 mL of water was filtered through a 0.45 μm filter paper. The filter paper was saved as the suspended sediment sample. A 30 mL sample was saved without treatment for analysis of anions. A 125 mL sample was acidified with 1-2 drops of 70% nitric acid and saved for cation analysis. Water and sediment samples were stored in a cooler until they were analyzed for alkalinity or transported to the University of Washington for analysis.

Samples were titrated in the field to determine the alkalinity. Approximately 150mL of water was filtered using the same system and 100ml was measured using a graduated cylinder and put in a glass beaker. The initial pH was measured and the sample was titrated with 0.1N HCl acid until it reached pH 4.5. Initial and final pH were recorded along with the volume of acid added. All samples were titrated within 4 hours of being sampled and immediately after filtration.

In the laboratory, the sediment samples were dried on the filter papers at 350 °C for 24 hours to remove water. The mass of the suspended sediment samples on the filter papers was measured on balance to an accuracy of 0.1 mg. The average mass of 20 individual filter papers was found to be 76.8 mg with a standard deviation of 0.5 mg. The weight of the filter paper was subtracted from the measurements of sediment on filter papers to obtain the mass of the sediment alone which was usually 2-5 times that of the filter paper.

Sediment samples were dissolved to determine the major and trace element composition of the suspended load. Fifty to 100 mg of sample was removed from the filter paper and weighed to a precision of 1 mg. The sample was placed in a tared graphite crucible that had been pre-ignited to a temperature of 250 °C and the weight was recorded. The sample and crucible were stored in a desiccation jar through the rest of the procedure. The sample was heated to 550 °C for 30 minutes to remove carbon and water and the weight was recorded. The difference in weights between the initial and post-heating is termed the loss on ignition and is assumed to be mainly organic matter.

The samples were fluxed in a ratio of about 1:5 with a 1:1 mixture of lithium metaborate and lithium tetraborate. The crucible and sample were heated to 900 °C for 15 minutes and the resulting bead was immediately dissolved in 5% ultrapure nitric acid. The samples were diluted appropriately and the major cations were measured with inductively coupled plasma atomic emission spectroscopy (ICP-AES) in the Chemistry Department of the University of Washington while Ge was measured as described below.

Major anions, (Cl^-, Br^-, SO_4^{2-}, PO_4^-, NO_3^-) were measured in the untreated dissolved load samples using ionic chromatography in the University of Washington's College of Forest Resources. Major cations (Al^{3+}, Ca^{2+}, K^+, Na^+, Fe^{2+}, Mg^{2+}, Mn^{2+}, Si^+) were measured in the acidified dissolved load sample and the fluxed suspended load sample using ICP-AES. The trace element Ge was measured using isotope-dilution and hydride generation followed by analysis on an ICP-MS by Dr. Louis Derry at Cornell University.

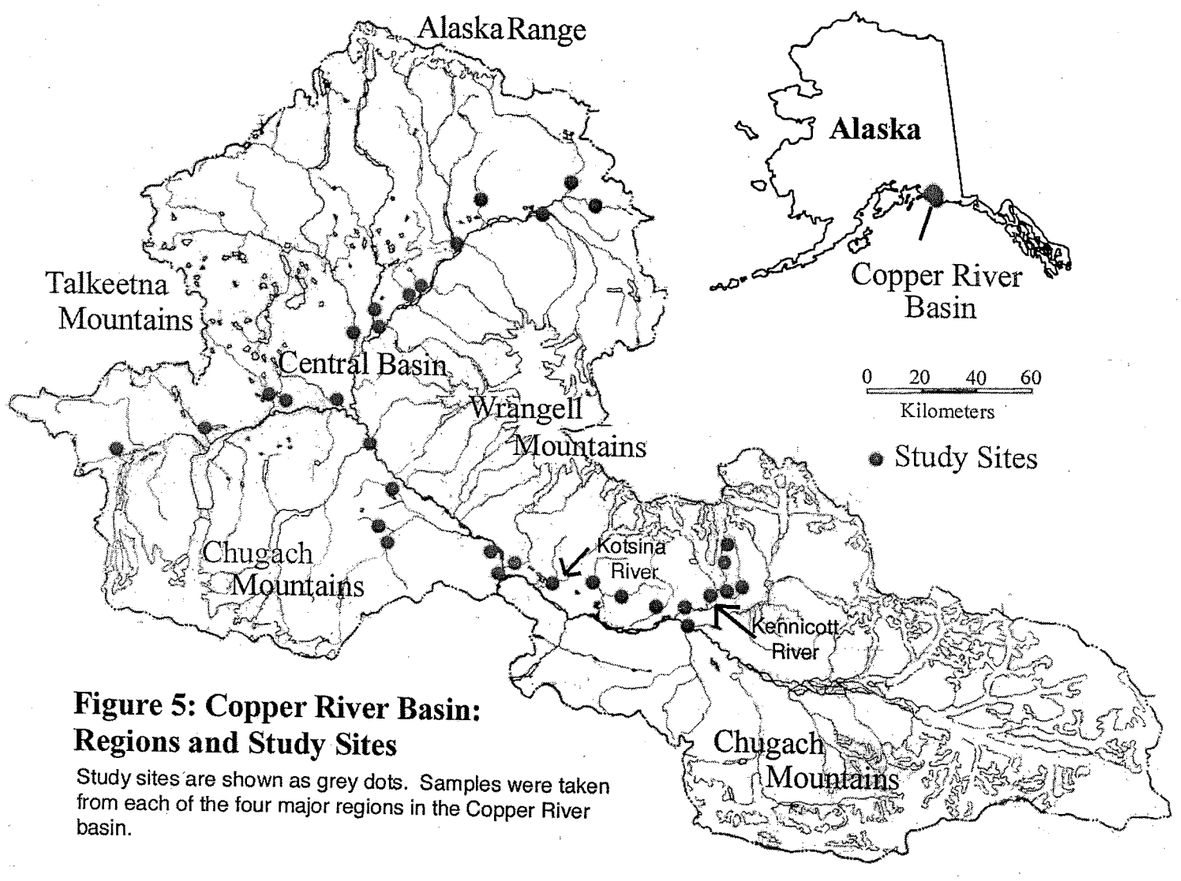

Figure 5: Copper River Basin: Regions and Study Sites

Study sites are shown as grey dots. Samples were taken from each of the four major regions in the Copper River basin.

Results and Discussion

THREE POPULATIONS OF RIVERS

The relationship between the Ge/Si ratio and 1/Si reveals that most of the rivers sampled fall on a mixing line of the form suggested by Murname and Stallard (1990) and are consistent with that found for Alaskan rivers by Froelich et al. (1992) (Figure 6). Two sets of river samples clearly deviate from this relationship: the Kennicott and Kotsina Rivers of the Wrangell Mountains have anomalously high Ge/SI ratios (5-12 pmol/μmol). In contrast, the Ge/Si ratio in the Matanuska River is low given its silicon concentration.

The Ge/Si ratios of the Kennicott and Kotsina Rivers are so high that a local mechanism controlling Ge/Si in these two rivers is invoked. These exceptional data are considered separately from the rest of the rivers, which show distinct characteristics based on the extent of glacier cover in the basins. I arbitrarily defined the glaciated basins to have 15% or more of their areas covered by ice; all other basins in the study area are considered periglacial. Given this definition, significant differences between the glacial and periglacial basins exist.

The Ge/Si ratio is higher in the glacial rivers than the periglacial rivers sampled. The difference is significant at the 0.005 level according to a non-parametric Mann-Whitney test. As discussed below, weathering intensity is not higher in these glacial rivers than the world average, rather, the Ge/Si ratio in these rivers reflects distinct glacial processes and not high weathering intensity as defined by Murname and Stallard (1990).

Glacial and periglacial rivers are also found to have distinctly different mass ratios of dissolved load to suspended load and distinct ratios of potassium to sodium. Glacial rivers have much larger suspended loads and somewhat lower dissolved loads, with higher K/Na ratios, than periglacial rivers (Figure 7and 8).

The Ge/Si ratios of glacial rivers sampled are high compared to world rivers and to the periglacial rivers sampled. These ratios may reflect two primary factors other than weathering intensity. The input of germanium-rich hydrothermal water to a few rivers in the Wrangell Mountains produces very high Ge/Si ratios in these rivers. The high Ge/Si ratios in the rest of the glacial rivers in the Copper River Basin are correlated with high K/Na ratios. Preferential

weathering of biotite is likely to be responsible for the high Ge/Si ratios in the other glacial rivers. Biotite weathering is cited as the cause of high K/Na ratios in glacial rivers (Stallard, 1995; Anderson et al., 1997). The disproportionate contribution of biotite to the dissolved load of glacial rivers is evident in the high $^{87}Sr/^{86}Sr$ ratios of glacial rivers in the Sierra Nevada Mountains (Blum et al., 1994). Moreover, biotite has a high Ge/Si ratio relative to continental crust (Bernstein, 1985; Filippelli et al., 2000) and Stallard (1995) predicted high Ge/Si ratios from glacial rivers due to the weathering of micas.

KENNICOTT-KOTSINA HOT SPRING

The high Ge/Si ratios in the Kennicott and Kotsina rivers and in the Copper River just downstream of the junction with the Kotsina are very likely result from hot spring input that is enriched in germanium. Hot springs are often enriched in germanium relative to silicon, exhibiting Ge/Si ratios up to three orders of magnitude higher than average rivers. One hot spring in the interior region of the Copper River basin was sampled in this study and the Ge/Si ratio of this water is 34 pmol/μmol. Ge/Si ratios well above 100 pmol/μmol have been observed in hot springs in the Himalaya (Derry, unpublished data).

In the Kennicott, Kotsina and Copper River just downstream of the junction with the Kotsina, germanium concentrations consistently correlate with concentrations of bicarbonate, sulfate, calcium, potassium, magnesium, sodium and silicon (Figure 9). These elements are commonly enriched in bicarbonate type thermal waters that exhibit low chloride concentrations and high bicarbonate and sulfate concentrations (Ellis and Mahon, 1977). A multiple linear regression yields a correlation coefficient of 0.9989 with most of the variance accounted for in bicarbonate, sodium, calcium and silicon concentrations. The Kennicott and Kotsina rivers show a negative correlation of K/Na versus Ge/Si that contrasts with the general positive trend in the other rivers (Figure 8).

An alternate hypothesis for very high Ge/Si ratios in the Kennicott River is the weathering of sulfide minerals, as germanium is know to be enriched in sulfide ores. Copper sulfides are present in the Kennicott basin and may weather subglacially or proglacially. To evaluate this hypothesis, a limited set of samples were analyzed for heavy metals. The Kennicott river is not characterized by very elevated Ba, Co, Cr, Cu, Li, Mn, Ti, or Zn compared to the neighboring McCarthy Creek and the Copper River (Table 2). Hence, high Ge/Si do not seem to be derived from sulfide mineral weathering. Moreover, sulfide mineral weathering does not

easily explain the association of germanium concentrations with concentrations of bicarbonate, magnesium, potassium, sodium and silicon.

BIOTITIE WEATHERING IN GLACIAL STREAMS

Biotite is frequently identified as the principal silicate mineral that weathers chemically in glacial environments (Blum et al., 1994; Blum and Erel, 1995; Anderson et al., 1997; Anderson et al., 2000). Biotite weathers more rapidly than most other silicate minerals; Blum et al. (1994) found biotite weathering 4 to 6 times as fast as plagioclase weathering in glacial streams of the Sierra Nevada Mountains. In addition, the sheet structure of biotite is susceptible to physical weathering to a greater extent that the more cross-linked silicates.

Biotite alteration is invoked as the cause of the high K/Na ratios in glacial rivers relative to other world rivers (Anderson et al., 1997). A positive association between K/Na and Ge/Si is apparent in the glacial rivers of the Copper River Basin (Figure 8). Biotite is also known to be enriched in Ge relative to Si with a ratio 3-4 times that of continental crust (Bernstein, 1985; Filippelli et al., 2000). The very early stages of biotite weathering are characterized by significant losses of K and Si and a relative increase in Na (Gilkes and Suddhipakarn, 1979; Pozzuoli et al., 1992; Burkins et al., 1999). It is reasonable, therefore, to assume that the weathering of biotite would release Ge along with K. The release of Ge relative to Si from biotite during the early stages of weathering has not been studied. Froelich et al., (1992) estimate that the globally averaged partitioning factor for Ge with respect to Si during incongruent weathering is 2.5, indicating that the Ge/Si of the first solute is about ¼ the Ge/Si of the rock. If this general partitioning factor holds for biotite weathering, a Ge/Si ratio of about 1 would be expected from the primary leachates. A study of the changes in the Ge/Si ratio in the solid and solute with progressive alteration of biotite is necessary to determine the specific Ge/Si ratio from this source. However, it seems reasonable that the high Ge/Si ratio of biotite will produce a relatively high Ge/Si in solution, even during the initial stages of alteration.

PERIGLACIAL RIVERS

The periglacial rivers do not show a very clear relationship between K/Na and Ge/Si. The increased presence of soils in these basins suggests that the processes partitioning and retaining germanium relative to silicon, including authigenic mineral formation, may significantly affect the Ge/Si of these rivers. In addition, although still dominantly subject to

physical weathering processes and low temperatures, diverse silicate minerals with variable Ge/Si and K/Na ratios are probably weathering.

The Ge/Si ratios of the Copper River Basin rivers spans the observed values for rivers worldwide (Figure 10). The periglacial rivers show a bimodal distribution with one cluster in the range for low weathering intensity headland streams and the other nearing values observed in the Amazon river. The glacial rivers show a very wide range of values with the bulk of the values at the high end of observed values or higher. As the Copper River enters the Pacific Ocean, it has a Ge/Si ratio of about 2 pmol/μmol – a value higher than average bedrock and higher than most of the unpolluted rivers of the world. The Copper River is probably controlled to some extent by the presence of high Ge/Si hydrothermal water, but part of this signal is due to the enhanced Ge/Si of the biotite-dominated glacial rivers. This result has several important implications for the current model of controls on the Ge/Si ratio of rivers and for the interpretation of the global record of germanium and silicon cycles.

FLUVIAL Ge/Si AND THE GLOBAL RECORD

Murname and Stallard's (1990) model of fluvial Ge/Si as a function of the weathering intensity is not appropriate for glaciated basins, as evident in the data from the Argentine Andes (Chillrud et al., 1994) and in the Copper River basin. Hence, the Ge/Si ratios in rivers do not simply reflect weathering intensity in all cases. I propose a new conceptual model of the chemical weathering reactions that control the Ge/Si of rivers, in which, an input from glacial chemical weathering is added to the incongruent weathering of primary minerals and the more congruent weathering of secondary minerals, as proposed by Murname and Stallard (1990) (Figure 11). The input from glacial chemical weathering is assumed to have the mean Ge/Si ratio and Si concentration of the glacial rivers of the Copper River basin. This composition is though to represent the dominance of biotite weathering in these basins.

The model is framed as an evolution in time from a glaciated system through deglaciation to a soil-forming environment and ultimately to an environment that allows the weathering of secondary clay minerals. A glacial system will be dominated by inputs from high Ge/Si biotite. The importance of this source will decrease in time after deglaciation as soil-forming, low Ge/Si incongruent weathering reactions of many primary silicate minerals become possible in the more stable, but still low weathering intensity environment. Finally, the high Ge/Si congruent weathering of secondary clays dominates the input. The transition between the

soil-forming and soil-weathering regimes is conceptually identical to Murname and Stallard's (1990) model of fluvial Ge/Si ratios. The most interesting element of this new model is the suggestion that the glacial runoff chemically resembles runoff from regions with considerable secondary mineral weathering than that dominated by primary mineral weathering, both characterized by relatively low Si concentrations and a high Ge/Si ratio. This similarity of the two end-members, physically- and chemically-dominated systems, has interesting implications for the interpretations of the glacial/interglacial ocean Ge/Si record.

Returning to the motivation for this study, namely, the oceanic record of changes in Ge/Si with climate, the new model of fluvial Ge/Si is used to evaluate changes in the contribution from glacial rivers to the ocean through a glacial-interglacial cycle. First, an estimate of the contribution of glacial weathering to the fluvial germanium and silicon flux to the ocean is made for an interglacial climate (Table 3). Secondly, the possible change in the glacial contribution to the total flux during glacial climates is considered along with the implications for the ocean Ge/Si record.

An estimate of the contribution of glacial weathering to the global fluvial Ge/Si ratio and flux is made using a characterization of glacial runoff based on the data from the Copper River basin and the estimates of the Si flux and Ge/Si ratio in the present climate. An estimate of the total discharge from temperate glaciers is the product of the surface area of temperate glaciers and the average accumulation rate – approximately 1000 km^3/yr. The silicon carried by this water is estimated to be present at a concentration of 59 μmol/L, the average concentration for the glacial rivers studied, for a total flux of 5.9×10^{10} mol Si/yr. from glacial weathering. The Ge/Si ratio of this flux is assumed to be 0.89, the average value of the glacial rivers studied (excluding the Kennicott and Kotsina Rivers). The global fluvial silicon flux of 6.2×10^{12} mol Si/yr. is taken from Treguer et al. (1995) and the discharge-weighted average Ge/Si ratio of this flux is assumed to be 0.54 (Froelich, Blanc et al., 1992). Given the estimates for the total flux and ratio and the glacial contribution, the contributions from primary mineral weathering and secondary mineral weathering can be determined (Table 3).

To estimate how the input from glacial weathering may have changed the total glacial fluvial Ge/Si ratio, I assumed that the input from glacial weathering during glacial periods was ten times the interglacial value and held the other fluxes constant. In this scenario, the total fluvial Ge/Si is 0.57 – higher than the interglacial value. In addition, the fractional contribution of glacial weathering to the global fluvial silicon flux is much larger than during interglacials. While this estimate of the importance of the glacial weathering silicon flux is crude, some

important conclusions can be made. First, the high Ge/Si ratio flux of silicon from glacial weathering does not help explain the low Ge/Si values of the glacial ocean. Even if the flux from glacial weathering were decreased during glacial periods relative to the fluxes from other fluvial sources, a scenario which seems unlikely, the relative importance of this contribution is so small today that decreasing it alone will not yield a low Ge/Si fluvial flux. The whole-ocean changes in Ge/Si could be related to the changing importance of primary silicate weathering relative to both glacial and secondary weathering, or, more likely, to changes in the sources and size of the dust flux to the ocean – a potentially significant and unquatified source.

Table 2: Heavy Metal Concentrations in the Kennicott River, McCarthy Creek and the Copper River

River	Concentration μg/L								pmol/L
	Ba	Co	Cr	Cu	Li	Mn	Ti	Zn	Ge
Kennicott River (glacial)	52.6	4.65	7.10	10.23	3.78	1.38	23.4	5.41	1.29×10^{-4}
McCarthy Creek (periglacial neighbor to Kennicott)	27.2	3.37	6.24	12.96	4.30	2.61	25.6	7.98	5.16×10^{-5}
Copper River (whole basin)	42.1	3.48	6.99	19.26	3.65	3.08	24.2	12.2	1.17×10^{-4}

Table 3: Estimates of the Contribution of Glacial Weathering to the Fluvial Flux During Glacial and Interglacial Periods

	Glacial Weathering	Primary Weathering	Secondary Weathering	Total
Interglacial Si Flux ($x10^{10}$ mol/yr.)	5.9	574	40	620
Interglacial Ge/Si (pmol/μmol)	0.89	0.33	3.5	0.54
Interglacial Contribution to Total Fluvial Si Flux	1%	93%	6%	100%
Glacial Si Flux ($x10^{10}$ mol/yr.)	59	574	40	673
Glacial Ge/Si (pmol/μmol)	0.89	0.33	3.5	0.57
Glacial Contribution to Total Fluvial Si Flux	9%	85%	6%	100%

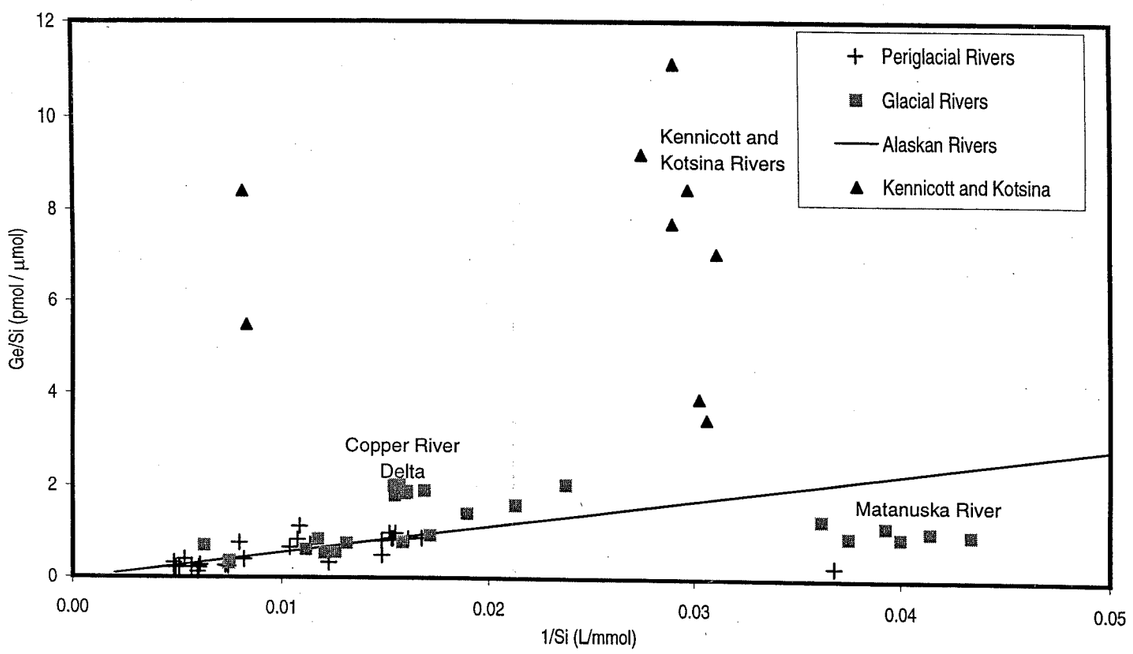

FIGURE 6: Ge/Si vs. 1/Si in Glacial and Periglacial Rivers
Most glacial and periglacial rivers in the Copper River Basin fall on the mixing line for Alaskan rivers defined by Froelich et al. (1992). Glacial rivers plot closer to the high weathering intensity endmember than periglacial rivers due to the high Ge/Si input of biotite weathering. The Kennicott and Kotsina Rivers deviate from other Alaskan rivers because they have high Ge/Si hydrothermal input.

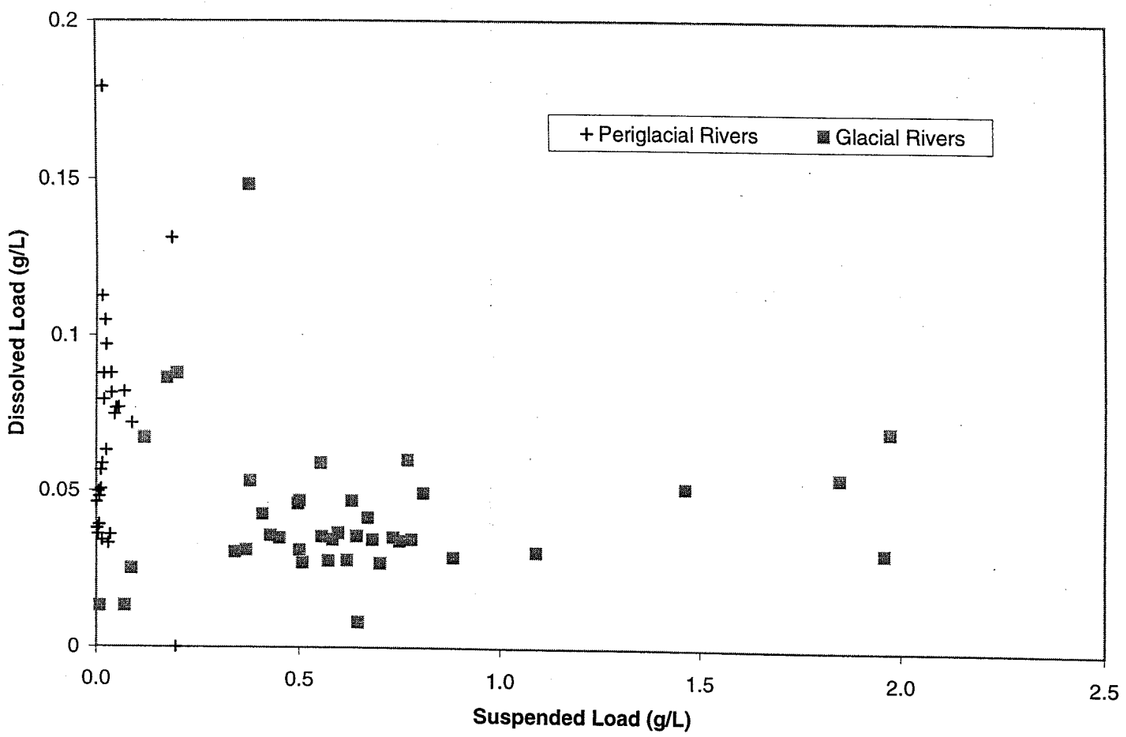

FIGURE 7: Dissolved and Suspended Loads of Glacial and Periglacial Rivers, Copper River Basin
Glacial and Periglacial Rivers in the Copper River Basin are distinct populations. Glacial rivers have much larger suspended loads and relatively small dissolved loads compared to periglacial rivers.

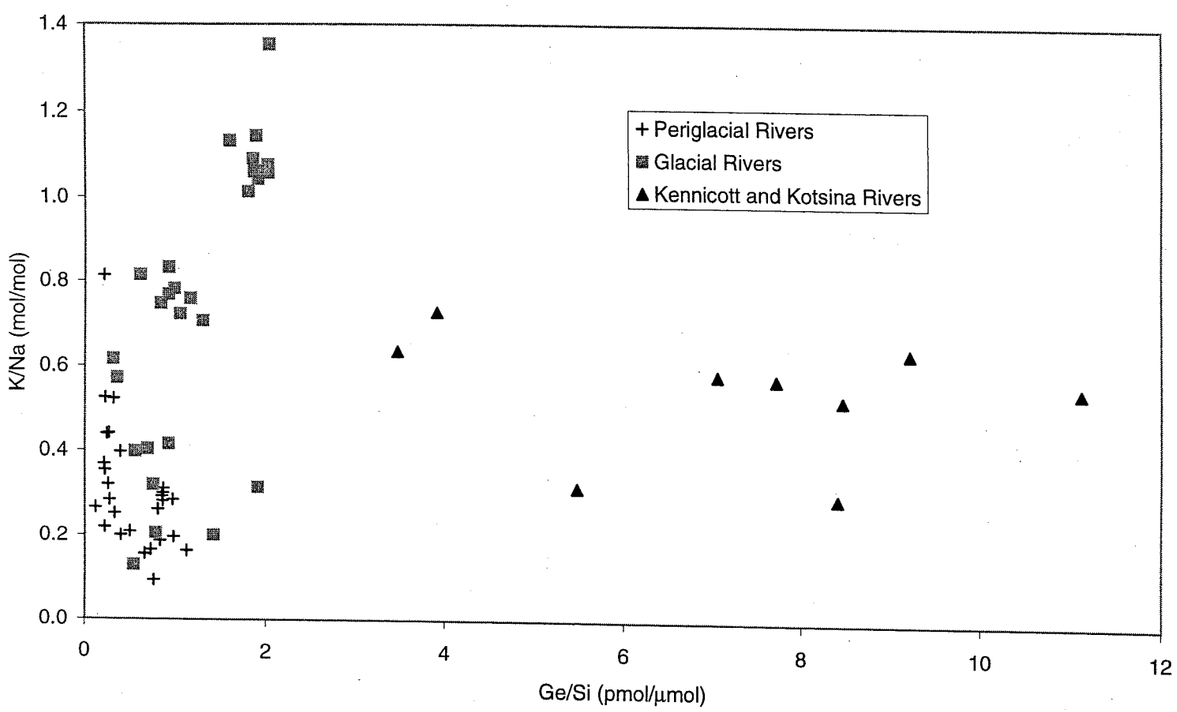

FIGURE 8: K/Na and Ge/Si of Glacial, Periglacial and Kennicott-Kotsina Rivers
The Kennicott and Kotsina Rivers have a distinct low K/Na, high Ge/Si input not present in the other rivers. Glacial rivers have a high K/Na and high Ge/Si input from biotite weathering. Most world rivers have a Ge/Si ratio less than 0.8. Periglacial rivers lack a distinct trend due to the mixing of Ge/Si and K/Na from several minerals.

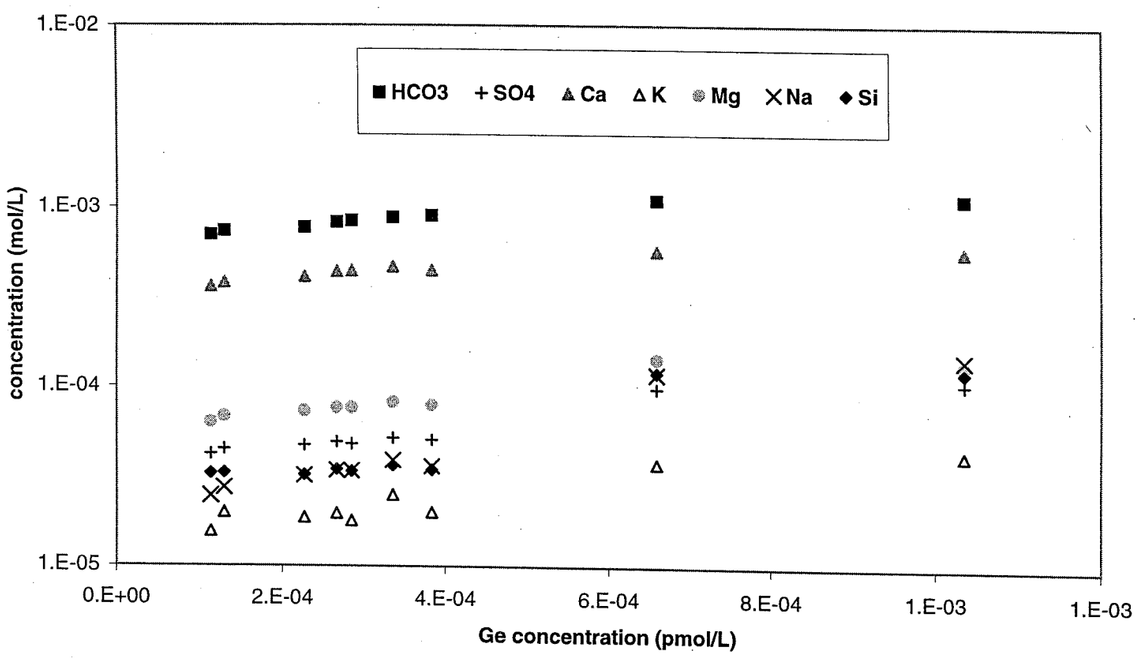

FIGURE 9: Chemistry of the Kennicott and Kotsina Rivers
Bicarbonate, sulfate, calcium, potassium, magnesium, sodium and silicon all vary systematically with germanium in these rivers

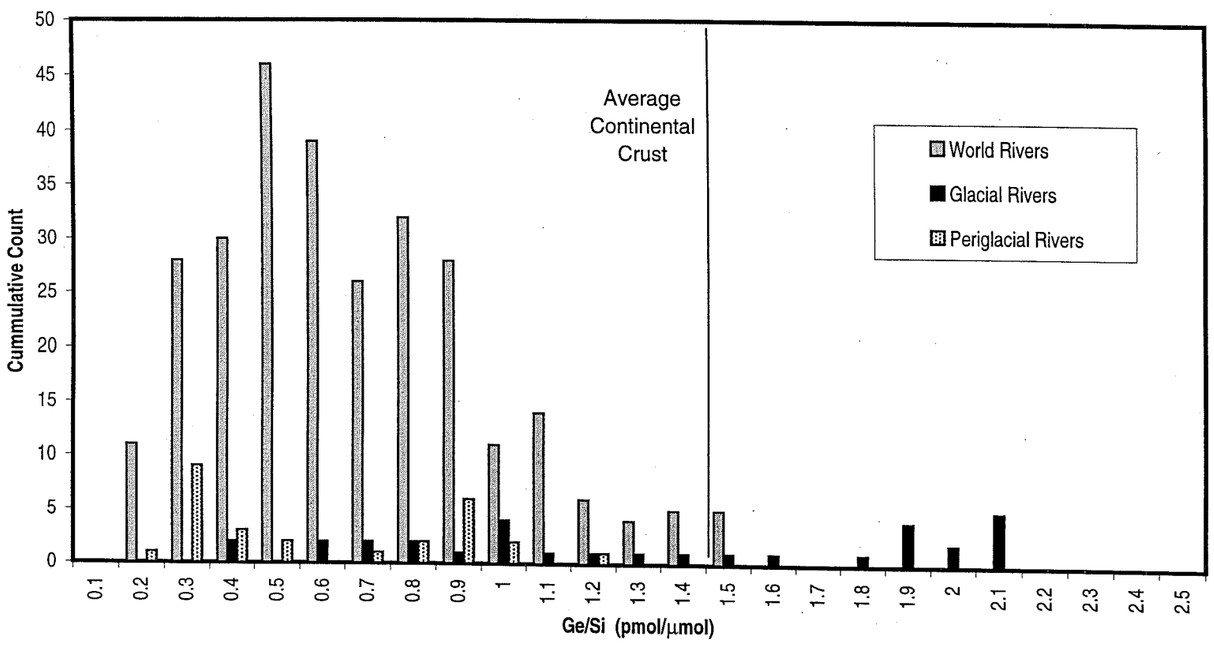

FIGURE 10: Fluvial Ge/Si Ratios in the Copper River Basin as Compared to World Rivers
The number of world rivers observed to have a given (Ge/Si) ratio, modified from Froelich et al. (1992). World rivers cluster well around the discharge-weighted mean of 0.54. Periglacial rivers studied have a bimodal distibution, the low end representing low intensity weathering and the high group dominated by biotite weathering. The glacial rivers nearly span the range of values for world rivers and many have a higher ratio than the average continental crust. The Kennicott and Kotsina Rivers are not shown on this plot.

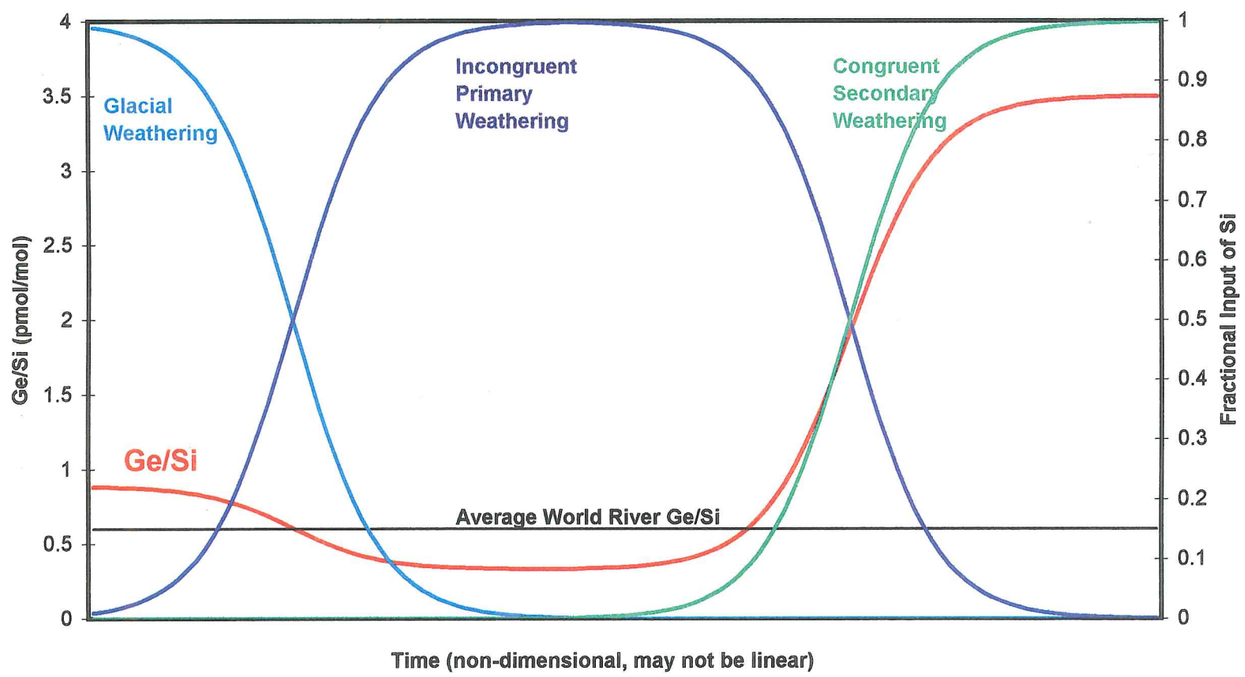

FIGURE 11: A new conceptual model of fluvial Ge/Si
The evolution of fluvial Ge/Si in time with changing inputs from glacial, incongruent primary (low intensity) and congruent secondary (high intensity) weathering is shown. The Ge/Si is given on the left axis, the fraction of silicon from each source is shown on the right. The average world river Ge/Si provided for reference. Murname and Stallard's (1990) model represents the transition from low to high intensity weathering and is conceptually identical to the right half of this figure. Rivers sampled in this study fall on the left half of the figure.

SUMMARY AND CONCLUSIONS

The major conclusion of this study is that, in the Copper River basin, the disproportionate contribution of biotite weathering to the dissolved loads of glacial rivers leads to relatively high Ge/Si ratios that are correlated with increases of the K/Na ratios and are independent of weathering intensity. This finding suggests that an expanded model of the controls on fluvial Ge/Si ratios that includes a contribution from glacial weathering of Ge-rich minerals, along with the contributions from incongruent weathering of primary minerals and more congruent weathering of secondary mineral suggested by Murname and Stallard (1990). High Ge/Si ratios are characteristic of from temperate glacier weathering, and hence do not directly help explain the low Ge/Si ratio of the ocean during glacial periods.

The dominance of biotite weathering in controlling the Ge/Si of glacial rivers underscores the importance of trace phases in controlling the chemistry of glacial weathering. This phenomenon has also been implicated in creating the high $^{87}Sr/^{86}Sr$ ratios of glacial rivers in the Sierra Nevada and in changing the ocean record of $^{87}Sr/^{86}Sr$ during the Quaternary (Blum et al., 1994; Blum and Erel, 1995). If the uniqueness of glacial river chemistry is found to be robust, the potential that various chemical markers of glaciation, including Ge/Si ratios, exist is high and their use in creating records of past climates and weathering rates on many temporal and spatial scales may prove to be a rich area of future research.

LIST OF REFERENCES

Anderson, S. P., J. I. Drever, C. D. Frost and P. Holden (2000). "Chemical weathering in the foreland of a retreating glacier." Geochimica et Cosmochimica Acta **64**(7): 1173-1189.

Anderson, S. P., J. I. Drever and N. F. Humphrey (1997). "Chemical weathering in glacial environments." Geology **25**(5): 399-402.

Archer, D., A. Winguth, D. Lea and N. Mahowald (2000). "What caused the glacial/interglacial atmospheric pCO_2 cycles." Reviews of Geophysics **38**(2): 159-189.

Bareille, G., M. Labracherie, R. A. Mortlock, E. Maier-Reimer and P. N. Froelich (1998). "A test of (Ge/Si)opal as a paleorecorder of (Ge/Si)seawater." Geology **26**(2): 179-182.

Bernstein, L. R. (1985). "Germanium geochemistry and mineralogy." Geochimica et Cosmochimica Acta **49**: 2409-2422.

Bernstien, L. R. and G. A. Waychunas (1987). "Germanium crystal chemistry in hematite and goethite from the Apex Mine, Utah, and some new data on germanium in aqueous solution and in stottite." Geochimica et Cosmochimica Acta **51**: 623-630.

Blum, J. D. and Y. Erel (1995). "A silicate weathering mechanism linking increases in marine $^{87}Sr/^{86}Sr$ with global glaciation." Nature **373**(6513): 415-418.

Blum, J. D., Y. Erel and K. Brown (1994). "$^{87}Sr/^{86}Sr$ ratios of Sierra Nevada stream waters: Implications for relative mineral weathering rates." Geochimica et Cosmochimica Acta **58**: 5019-5025.

Broecker, W. A. and T. H. Peng (1982). Tracers in the Sea, Palisades, NY, Lamont-Doherty Geological Observatory.

Brown, G. H., M. J. Sharp, M. Tranter, A. M. Gurnell and P. W. Nienow (1994). "Impact of post-mixing chemical reactions on the major ion chemistry of bulk meltwaters draining the Haut Glacier D'Arolla Valais, Switzerland." Hydrological Processes **8**: 465-480.

Brown, G. H., M. Tranter and M. J. Sharp (1996). "Experimental investigations of the weathering of suspended sediment by alpine glacial meltwater." Hydrological Processes **10**: 579-597.

Burkins, D. L., J. D. Blum, K. Brown, R. C. Reynolds and Y. Erel (1999). "Chemistry and mineralogy of a granitic, glacial soil chronosequence, Sierra Nevada Mountains, California." Chemical Geology **162**: 1-14.

Burton, J. D., F. Culkin and J. P. Riley (1959). "The abundances of gallium and germanium in terrestrial materials." Geochimica et Cosmochimica Acta **16**: 151-180.

Chillrud, S. N., F. L. Pedrozo, P. F. Temporetti, H. F. Planas and P. N. Froelich (1994). "Chemical weathering of phosphate and germanium in glacial meltwater streams: Effects of subglacial pyrite oxidation." Limnology and Oceanography **39**(5): 1130-1140.

Collins, D. N. (1995). "Dissolution kinetics, transit times through subglacial hydrological pathways and diurnal variations of solute content of meltwaters draining from an alpine glacier." Hydrological Processes **9**: 897-910.

Drever, J. I. and D. R. Hurcomb (1986). "Neutralization of atmospheric acidity by chemical weathering in an alpine drainage basin in the North Cascade Mountains." Geology **14**: 221-224.

Elderfield, H. and A. Schultz (1996). "Mid-ocean ridge hydrothermal fluxes and the chemical composition of the ocean." Annual Review of Earth and Planetary Sciences **24**: 191-224.

Ellis, A. J. and W. A. J. Mahon (1977). Chemistry and Geothermal Systems. New York, Academic Press.

Fairchild, I. J., J. S. Killawee, M. J. Sharp, B. Spiro, B. Hubbard, R. D. Lorrain and J.-L. Tison (1999). "Solute generation and transfer from a chemically reactive alpine glacial-periglacial system." Earth Surface Processes and Landforms **24**: 1189-1211.

Filippelli, G. M., J. W. Carnahan, L. A. Derry and A. Kurtz (2000). "Terrestrial paleorecords of Ge/Si cycling derived from lake diatoms." Chemical Geology **168**: 9-26.

Froelich, P. N. and M. O. Andreae (1981). "The marine geochemistry of Germanium: Ekasililcon." Science **213**: 205-207.

Froelich, P. N., V. Blanc, R. A. Mortlock and S. N. Chillrud (1992). "River fluxes of dissolved silica to the ocean were higher during glacials: Ge/Si in diatoms, rivers and oceans." Paleoceanography **7**(6): 739-767.

Froelich, P. N., G. A. Hambrick, M. O. Andreae, R. A. Mortlock and J. M. Edmond (1985). "The geochemistry of inorganic germanium in natural waters." Journal of Geophysical Research **90**(C1): 1133-1141.

Gibbs, M. T. and L. R. Kump (1994). "Global chemical erosion during the last glacial maximum and the present: sensitivity to changes in lithology and hydrology." Paleoceanography **9**: 529-543.

Gilkes, R. J. and A. Suddhipakarn (1979). "Biotite alteration in deeply weathered granite. I. Morphological, mineralogical, and chemical properties." Clays and Clay Minerals **27**(5): 349-360.

Hallet, B., L. Hunter and J. Bogen (1996). "Rates of erosion and sediment evacuation by glaciers: A review of field data and their implications." Global and Planetary Change **12**: 213-235.

Harbor, J. and J. Warburton (1993). "Relative rates of glacial and nonglacial erosion in alpine environments." Arctic and Alpine Research **25**(1): 1-7.

King, S. L., P. N. Froelich and R. A. Jahnke (2000). "Early diagenesis of germanium in sediments of the Antarctic South Atlantic: In search of the missing Ge sink." Geochimica et Cosmochimica Acta **64**(8): 1375-1390.

Kump, L. R. and R. B. Alley (1994). Global chemical weathering on glacial time scales. Material Fluxes on the Surface of the Earth, National Academy Press: 46-60.

Kurtz, A. C. and L. A. Derry (1998). Mineral aerosols and the marine silica cycle: constraints from Ge/Si. GSA Annual Meeting, Salt Lake City, Geological Society of America.

Mortlock, R. A., P. N. Froelich, R. A. Feely, G. J. Massoth, D. A. Butterfield, J. E. Lupton (1993). "Silica and germanium in Pacific Ocean hydrothermal vents and plumes." Earth and Planetary Science Letters **119**(3): 365-378.

Mortlock, R. A., and P. N. Froelich (1987). "Continental weathering of germanium; Ge/Si in the global river discharge." Geochimica et Cosmochimica Acta **51**(8): 2075-2082.

Munhoven, G. and L. M. Francois (1996). "Glacial-interglacial variability of atmospheric CO_2 due to changing continental silicate rock weathering: A model study." Journal of Geophysical Research **101(D16)**: 21423-21437.

Murname, R. J. and R. F. Stallard (1990). "Germanium and silicon in rivers of the Orinoco drainage basin." Nature **344**: 749-752.

Nokleberg, W. J., G. Plafker and F. H. Wilson (1994). Geology of south-central Alaska. The Geology of Alaska, The Geological Society of America. **G-1:** 311-366.

Petit, J. R., et al., (1999). "Climate and atmospheric history of the past 420,000 years from the Vostok ice core, Antarctica." Nature **399**: 429-436.

Pozzuoli, A., E. Vila, E. Franco, A. Ruiz-Amil and C. De La Calle (1992). "Weathering of biotite to vermiculite in Quaternary lahars from Monti Ernici, central Italy." Clay Minerals **27**: 175-184.

Raiswell, R. and A. G. Thomas (1984). "Solute acquisition in glacial melt waters. I. Fjallsjokull (South-east Iceland): bulk melt waters with closed-system characteristics." Journal of Glaciology **30**(104): 35-43.

Reynolds, R. C. and N. M. Johnson (1972). "Chemical weathering in the temperate glacial environment of the Northern Cascade mountains." Geochimica et Cosmochimica Acta **36**: 537-554.

Ruddiman, W. F., M. E. Raymo, W. L. Prell and J. E. Kutzbach (1997). The Uplift-Climate Connection: A Synthesis. Tectonic Uplift and Climate Change. W. F. Ruddiman. New York, Plenum Press: 471-515.

Sharp, M., M. Tranter, G. H. Brown and M. Skidmore (1995). "Rates of chemical denudation and CO2 drawdon in a glacier-covered alpine catchment." Geology **23**(1): 61-64.

Souchez, R. A. and M. M. Lemmens (1987). Solutes. Glacio-fluvial sediment transfer: An alpine perspective. A. M. Gurnell and M. J. Clark. New York, John Wiley: 285-303.

Stallard, R. F. (1995). "Tectonic, environmental, and human aspects of weathering and erosion: A global review using a steady-state perspective." Annual Reviews of Earth and Planetary Science **23**: 11-39.

Tranter, M., G. Brown, R. Raiswell, M. Sharp and A. Gurnell (1993). "A conceptual model of solute acquisition by Alpine glacial meltwaters." Journal of Glaciology **39**(133): 573-581.

Treguer, P., D. M. Nelson, A. J. Van Bennekom, D. J. DeMaster, A. Leynaert and B. Queguiner (1995). "The silica balance in the world ocean." Science **268**: 375-379.

Zhou, L. and F. T. Kyte (1991). "Are there any significant sinks in the marine Ge cycle other than biogenic opal?" Eos **72**: 263-264.

Appendix A: Water Sample Chemistry

Site Number	Site Name	Region	Type	pH	HCO_3 mol/L	Sediment Load g/L	Fe mol/L	Br mol/L	Al mol/L	PO_4 mol/L
1-A	Childs Glacier	Entire basin	Glacial	8.27	1.42E-03	0.43	6.07E-07	0	2.43E-06	0
1-B	Childs Glacier	Entire basin	Glacial	8.24	1.59E-03	0.56	8.39E-07	0	2.39E-06	0
1-C	Childs Glacier	Entire basin	Glacial	7.87	1.00E-03	0.60	7.32E-07	1.25E-07	2.04E-06	3.26E-07
2	Hotcakes	Entire basin	Glacial	8.30	2.03E-03	0.75	8.21E-07	0	2.25E-06	0
3	Long Island	Entire basin	Glacial	8.31	1.99E-03	0.68	9.64E-07	0	2.79E-06	0
4	Delta Backwater	Entire basin	Glacial	8.39	1.52E-03	0.45	7.32E-07	0	1.75E-06	2.74E-07
5	Flag Point	Entire basin	Glacial	8.30	2.81E-03	0.78	8.93E-07	7.51E-08	2.14E-06	0
6	Alaganik Slough	Chugach Mtns.	Glacial	7.07	7.65E-04	0.01	1.30E-06	0	0	1.05E-07
7	Sheridan River	Chugach Mtns.	Glacial	6.94	7.45E-04	0.07	1.20E-06	1.13E-07	1.00E-06	2.63E-07
8	Western Delta	Entire basin	Glacial	8.27	2.45E-03	0.73	1.25E-06	0	2.86E-06	0
9	West Delta	Entire basin	Glacial	8.00	9.95E-04	0.64	1.18E-06	8.76E-08	2.96E-06	4.42E-07
10	Little Nelchina	Chugach Mtns.	Periglacia	8.01	1.75E-03	0.19	9.46E-07	0	1.50E-06	0
11	Mud Springs	Interior	Spring	7.04	1.73E-03	0.20	3.89E-06	4.39E-04	9.68E-06	5.74E-06
12	Tolsona Ck.	Interior	Periglacia	8.01	1.43E-03	0.02	3.48E-06	2.93E-06	1.79E-06	0
13	Tazlina Ck.	Chugach Mtns.	Glacial	7.95	9.27E-04	0.41	7.50E-07	2.13E-07	1.93E-06	0
14	Klutina R.	Chugach Mtns.	Glacial	7.93	8.31E-04	0.34	7.86E-07	1.75E-07	1.46E-06	0
15	Willow Ck.	Chugach Mtns.	Periglacia	7.90	2.92E-03	0.02	5.16E-06	0	1.46E-06	0
16	Squirrel Ck.	Chugach Mtns.	Periglacia	7.96	1.13E-03	0.03	8.93E-07	0	1.32E-06	1.05E-07
17	Tonsina R.	Chugach Mtns.	Glacial	7.83	7.36E-04	0.09	1.11E-06	0	2.04E-06	0
18	Chitina's Copper R.	Most of the Basi	Glacial	8.09	1.10E-03	0.81	9.46E-07	1.25E-07	5.75E-06	0
19	Kotsina R.	Alaska Range	Glacial	8.11	1.13E-03	1.46	9.64E-07	1.63E-07	6.21E-06	1.35E-06
20	Strelna Ck.	Alaska Range	Periglacia	8.16	2.47E-03	0.02	3.93E-07	0	1.00E-06	0
21	Choksona R.	Alaska Range	Periglacia	8.17	1.95E-03	0.02	2.86E-07	0	0	0
22	Gilahina R.	Alaska Range	Periglacia	8.03	1.44E-03	0.02	3.75E-07	3.63E-07	5.71E-07	0
23	Lakina R.	Alaska Range	Glacial	8.06	1.42E-03	0.12	2.86E-07	1.90E-06	1.79E-06	0
24-A	Clear Ck.	Wrangell Mtns.	Spring	7.65	3.18E-03	0.02	1.25E-07	2.63E-07	1.79E-06	0
24-B	Clear Ck.	Wrangell Mtns.	Spring	7.89	3.92E-03	0.01	1.79E-07	4.51E-07	1.46E-06	0
25-A	Kennicott R.	Wrangell Mtns.	Glacial	8.40	8.97E-04	0.50	4.29E-07	3.63E-07	2.21E-06	0
25-B	Kennicott R.	Wrangell Mtns.	Glacial	8.25	7.69E-04	0.50	3.04E-07	5.01E-07	1.96E-06	9.26E-07
25-C	Kennicott R.	Wrangell Mtns.	Glacial	8.44	8.24E-04	0.50	3.93E-07	0	2.43E-06	2.11E-07
25-D	Kennicott R.	Wrangell Mtns.	Glacial	8.51	8.73E-04	0.37	3.39E-07	0	2.54E-06	0
25-E	Kennicott R.	Wrangell Mtns.	Glacial	8.48	8.38E-04	0.58	3.57E-07	2.38E-07	2.21E-06	0
25-F	Kennicott R.	Wrangell Mtns.	Glacial	8.62	7.00E-04	0.63	5.71E-07	4.76E-07	2.79E-06	2.11E-08
25-G	Kennicott R.	Wrangell Mtns.	Glacial	8.59	7.34E-04	0.55	4.11E-07	9.89E-07	2.50E-06	4.42E-07

Appendix A: Water Sample Chemistry, cont.

Site Number	Site Name	Region	Type	pH	HCO_3 mol/L	Sediment Load g/L	Fe mol/L	Br mol/L	Al mol/L	PO_4 mol/L
26-A	McCarthy Ck.	Wrangell Mtns.	Periglacia	8.06	1.71E-03	0.06	2.86E-07	0	1.46E-06	6.32E-08
26-B	McCarthy Ck.	Wrangell Mtns.	Periglacia	8.25	1.72E-03	0.07	8.93E-08	0	1.68E-06	0
26-C	McCarthy Ck.	Wrangell Mtns.	Periglacia	8.19	1.73E-03	0.04	8.93E-08	0	1.46E-06	0
26-D	McCarthy Ck.	Wrangell Mtns.	Periglacia	7.96	1.63E-03	0.05	2.32E-07	0	1.04E-06	0
26-E	McCarthy Ck.	Wrangell Mtns.	Periglacia	8.33	1.68E-03	0.05	1.43E-07	0	1.46E-06	9.47E-08
26-F	McCarthy Ck.	Wrangell Mtns.	Periglacia	7.89	1.57E-03	0.09	1.61E-07	0	1.46E-06	0
27	Jumbo Ck.	Wrangell Mtns.	Periglacia	8.17	1.43E-03	0.00	1.96E-07	0	3.57E-07	0
28	Bonanza Ck.	Wrangell Mtns.	Periglacia	8.16	1.52E-03	0.01	1.61E-07	0	6.07E-07	2.11E-07
29	Chitina R.	Chugach Mtns.	Glacial	8.24	8.82E-04	1.96	9.82E-07	0	3.71E-06	0
30	Porcupine Ck.	Alaska Range	Periglacia	8.07	1.96E-03	0.02	1.96E-07	0	7.14E-07	4.00E-07
31	Athell Ck.	Alaska Range	Periglacia	7.65	1.17E-03	0.01	4.29E-07	0	1.07E-06	0
32	Slana's Copper R.	Wrangell Mtns.	Glacial	7.97	1.74E-03	0.20	5.18E-07	0	2.46E-06	0
33	Slana R.	Alaska Range	Glacial	8.11	1.77E-03	0.17	5.54E-07	0	1.21E-06	0
34	Indian Ck.	Alaska Range	Periglacia	7.88	1.19E-03	0.03	2.86E-07	0	1.32E-06	1.18E-06
35	Chistochina R.	Alaska Range	Glacial	8.13	1.35E-03	1.97	1.36E-06	1.13E-07	2.54E-06	0
36	Sinona Ck.	Interior	Periglacia	7.98	1.69E-03	0.00	1.00E-06	0	1.43E-06	0
37	Tulsona R.	Interior	Periglacia	8.16	2.06E-03	0.01	3.59E-06	0	1.61E-06	1.21E-06
38	Gakona R.	Alaska Range	Glacial	8.19	1.38E-03	1.85	5.71E-07	0	2.29E-06	0
39	Gakona's Copper R.	Wrangell Mtns.	Glacial	8.10	1.22E-03	0.77	9.64E-07	0	4.50E-06	0
40	Gulkana R.	Interior	Periglacia	8.12	1.26E-03	0.01	1.80E-06	8.76E-08	1.93E-06	0
41	Lake Louise	Interior	Periglacia	7.75	1.23E-03	0.00	4.11E-07	2.88E-07	1.57E-06	6.74E-07
42	Mendeltna R.	Interior	Periglacia	8.17	1.73E-03	0.01	9.64E-07	0	1.21E-06	4.21E-07
43-A1	Matanuska - big station	Chugach Mtns.	Glacial	8.40	4.99E-04	0.88	1.32E-06	0	5.54E-06	4.84E-07
43-A2	Matanuska - big station	Chugach Mtns.	Glacial	8.22	4.98E-04	1.09	6.07E-07	0	3.36E-06	0
43-B	Matanuska - Mammoth vent	Chugach Mtns.	Glacial	8.26	4.93E-04	0.57	7.14E-07	0	3.00E-06	0
43-D	Matanuska - culvert	Chugach Mtns.	Glacial	8.39	5.14E-04	0.51	1.18E-06	0	5.54E-06	0
43-E	Matanuska - North Vent	Chugach Mtns.	Glacial	8.10	5.05E-04	0.62	6.96E-07	0	3.71E-06	7.37E-08
43-F	Matanuska -main drag	Chugach Mtns.	Glacial	8.00	4.96E-04	0.70	8.39E-07	0	3.14E-06	0
44	Matanuska R - King Mtn.	Chugach Mtns.	Glacial	8.06	1.04E-03	0.38	4.11E-07	0	3.25E-06	0
45	Matanuska - Hick's Ck.	Chugach Mtns.	Glacial	8.31	2.44E-03	0.38	4.82E-07	0	2.29E-06	0
46	Liberty Ck.	Chugach Mtns.	Periglacia	7.74	6.12E-04	0.01	8.93E-08	1.28E-06	1.21E-06	0
47	Clear Ck. (footbridge)	Wrangell Mtns.	Spring	7.62	2.94E-03	0.04	5.18E-07	7.51E-08	1.93E-06	0
48	Nizina R.	Wrangell Mtns.	Glacial	8.21	1.24E-03	0.67	6.07E-07	0	3.00E-06	0

Appendix A: Water Sample Chemistry, cont.

Site Number	NO_3 mol/L	SO_4 mol/L	Ca mol/L	Cl mol/L	K mol/L	Mg mol/L	Mn mol/L	Na mol/L	Si mol/L	Ge pmol/L	Ge/Si pmol/μmol
1-A	1.35E-06	6.04E-05	4.78E-04	7.37E-05	5.53E-05	1.09E-04	1.64E-07	5.45E-05	6.46E-05	1.17E-04	1.80
1-B	1.58E-06	5.86E-05	4.63E-04	8.87E-05	5.76E-05	1.08E-04	2.18E-07	5.03E-05	6.23E-05	1.18E-04	1.89
1-C	2.11E-06	5.92E-05	4.75E-04	1.02E-04	5.75E-05	1.09E-04	1.64E-07	5.27E-05	6.27E-05	1.16E-04	1.86
2	1.77E-06	5.88E-05	4.58E-04	6.25E-05	5.27E-05	1.06E-04	1.64E-07	4.97E-05	6.24E-05	1.16E-04	1.86
3	1.37E-06	6.02E-05	4.70E-04	5.11E-05	5.34E-05	1.10E-04	1.82E-07	5.11E-05	6.42E-05	1.23E-04	1.91
4	1.29E-06	5.78E-05	4.81E-04	5.23E-05	5.34E-05	1.06E-04	1.82E-07	7.57E-05	6.04E-05	1.12E-04	1.86
5	1.23E-06	6.02E-05	4.69E-04	5.13E-05	5.54E-05	1.11E-04	2.00E-07	5.20E-05	6.48E-05	1.29E-04	2.00
6	4.23E-06	1.95E-05	1.66E-04	5.68E-05	7.50E-06	1.38E-05	1.09E-07	1.92E-05	3.88E-05	8.01E-05	2.06
7	1.63E-06	2.41E-05	1.41E-04	4.45E-05	2.62E-05	2.30E-05	1.64E-07	2.31E-05	4.70E-05	7.52E-05	1.60
8	1.29E-06	6.01E-05	4.84E-04	5.31E-05	5.49E-05	1.12E-04	1.82E-07	5.10E-05	6.46E-05	1.31E-04	2.02
9	2.71E-06	6.01E-05	4.80E-04	6.52E-05	5.46E-05	1.10E-04	1.82E-07	5.16E-05	6.38E-05	1.29E-04	2.02
10	5.37E-06	5.70E-04	1.41E-03	3.74E-05	2.72E-05	2.87E-04	2.18E-07	2.92E-04	1.26E-04	9.54E-05	0.76
11	2.30E-04	1.16E-05	8.18E-03	3.27E-01	1.99E-03	1.06E-03	3.09E-05	1.77E-02	1.47E-04	5.03E-03	34.24
12	1.65E-06	7.82E-06	5.69E-04	1.11E-03	4.90E-05	2.10E-04	7.09E-07	2.62E-04	9.29E-05	7.69E-05	0.83
13	1.53E-06	6.52E-05	5.10E-04	2.49E-04	1.84E-05	9.85E-05	4.55E-07	9.10E-05	5.28E-05	7.47E-05	1.42
14	2.87E-06	3.68E-05	4.10E-04	1.48E-04	1.41E-05	7.50E-05	3.64E-07	3.40E-05	5.83E-05	5.40E-05	0.93
15	1.16E-06	1.19E-05	8.50E-04	1.34E-04	3.32E-05	3.85E-04	4.55E-07	9.33E-05	1.98E-04	4.37E-05	0.22
16	2.29E-06	1.78E-05	4.11E-04	1.36E-04	1.71E-05	1.40E-04	1.82E-07	4.64E-05	1.67E-04	3.54E-05	0.21
17	2.47E-06	2.71E-05	3.46E-04	9.91E-05	1.05E-05	6.20E-05	1.82E-07	2.64E-05	7.94E-05	4.41E-05	0.56
18	2.02E-06	9.81E-05	5.74E-04	1.60E-04	3.75E-05	1.44E-04	4.55E-07	1.18E-04	1.20E-04	6.59E-04	5.48
19	2.16E-06	1.06E-04	5.78E-04	1.67E-04	4.29E-05	1.34E-04	4.73E-07	1.45E-04	1.23E-04	1.03E-03	8.41
20	3.74E-06	7.77E-04	2.05E-03	6.78E-05	2.14E-05	5.62E-04	2.36E-07	1.30E-04	9.20E-05	1.03E-04	1.12
21	3.79E-06	3.64E-04	1.35E-03	7.49E-05	1.48E-05	3.30E-04	1.64E-07	8.92E-05	8.79E-05	6.39E-05	0.73
22	5.32E-06	9.86E-05	7.91E-04	3.65E-04	1.02E-05	1.43E-04	2.18E-07	5.09E-05	1.22E-04	4.83E-05	0.40
23	5.98E-06	1.19E-04	7.62E-04	4.50E-04	1.37E-05	2.03E-04	2.00E-07	4.28E-05	7.61E-05	5.74E-05	0.75
24-A	1.50E-05	1.08E-04	1.23E-03	2.45E-04	2.91E-05	3.95E-04	1.82E-07	1.33E-04	1.77E-04	3.86E-05	0.22
24-B	1.26E-05	9.23E-05	1.57E-03	5.84E-04	3.72E-05	4.37E-04	2.18E-07	9.35E-05	1.88E-04	7.39E-05	0.39
25-A	5.21E-06	5.08E-05	4.47E-04	5.12E-04	1.99E-05	7.90E-05	1.82E-08	3.60E-05	3.44E-05	3.83E-04	11.12
25-B	3.94E-06	4.71E-05	4.09E-04	6.01E-04	1.86E-05	7.30E-05	1.82E-08	3.19E-05	3.21E-05	2.27E-04	7.06
25-C	3.97E-06	4.92E-05	4.37E-04	1.16E-04	1.96E-05	7.62E-05	1.82E-08	3.41E-05	3.45E-05	2.67E-04	7.72
25-D	1.53E-06	5.18E-05	4.66E-04	6.55E-05	2.49E-05	8.20E-05	0.00E+00	3.90E-05	3.64E-05	3.35E-04	9.21
25-E	2.79E-06	4.80E-05	4.42E-04	2.13E-04	1.78E-05	7.62E-05	0.00E+00	3.38E-05	3.36E-05	2.85E-04	8.46
25-F	6.03E-06	4.20E-05	3.61E-04	6.83E-04	1.55E-05	6.32E-05	-1.82E-08	2.44E-05	3.26E-05	1.13E-04	3.47
25-G	5.95E-06	4.48E-05	3.79E-04	9.85E-04	1.98E-05	6.80E-05	0.00E+00	2.72E-05	3.30E-05	1.29E-04	3.92

Appendix A: Water Sample Chemistry, cont.

Site Number	NO_3 mol/L	SO_4 mol/L	Ca mol/L	Cl mol/L	K mol/L	Mg mol/L	Mn mol/L	Na mol/L	Si mol/L	Ge pmol/L	Ge/Si pmol/μmol
26-A	3.90E-06	2.40E-04	1.06E-03	1.09E-05	1.83E-05	2.83E-04	1.82E-08	6.40E-05	6.46E-05	6.25E-05	0.97
26-B	3.61E-06	2.78E-04	1.07E-03	2.83E-05	2.00E-05	2.86E-04	5.45E-08	6.62E-05	6.53E-05	5.62E-05	0.86
26-C	4.53E-06	2.44E-04	1.08E-03	9.73E-05	1.77E-05	2.88E-04	3.64E-08	6.74E-05	6.75E-05	5.44E-05	0.81
26-D	3.63E-06	2.33E-04	1.02E-03	2.12E-05	1.84E-05	2.72E-04	-1.82E-08	6.26E-05	6.21E-05	5.28E-05	0.85
26-E	3.79E-06	2.39E-04	1.05E-03	1.13E-05	1.84E-05	2.79E-04	0.00E+00	6.51E-05	6.51E-05	5.59E-05	0.86
26-F	4.03E-06	2.10E-04	9.82E-04	5.51E-05	1.90E-05	2.56E-04	-1.82E-08	6.10E-05	5.97E-05	5.16E-05	0.86
27	2.69E-06	2.26E-05	5.35E-04	1.12E-04	7.53E-06	2.14E-04	2.73E-07	3.82E-05	6.58E-05	6.43E-05	0.98
28	3.27E-06	2.16E-05	5.26E-04	5.78E-06	1.04E-05	2.41E-04	7.27E-08	6.63E-05	9.63E-05	6.32E-05	0.66
29	1.02E-06	5.41E-05	4.40E-04	3.42E-05	5.07E-05	1.08E-04	2.18E-07	3.75E-05	4.21E-05	8.62E-05	2.05
30	6.47E-06	2.93E-04	1.29E-03	6.55E-05	3.47E-05	3.14E-04	1.64E-07	7.89E-05	1.35E-04	3.29E-05	0.24
31	2.16E-06	1.44E-04	7.66E-04	3.09E-05	2.18E-05	1.73E-04	2.91E-07	4.94E-05	1.65E-04	4.41E-05	0.27
32	1.92E-06	2.76E-04	1.06E-03	3.77E-05	4.14E-05	4.42E-04	2.36E-07	7.24E-05	1.34E-04	4.76E-05	0.36
33	1.77E-06	2.72E-04	1.04E-03	2.94E-05	4.26E-05	4.30E-04	4.73E-07	6.92E-05	1.34E-04	4.21E-05	0.31
34	4.03E-07	3.32E-05	5.28E-04	6.09E-06	2.30E-05	1.40E-04	2.00E-07	4.38E-05	2.08E-04	4.71E-05	0.23
35	1.56E-06	1.90E-04	8.30E-04	1.81E-04	3.73E-05	2.81E-04	2.18E-07	4.57E-05	8.96E-05	5.47E-05	0.61
36	8.39E-07	1.49E-05	6.56E-04	1.13E-04	4.48E-05	2.36E-04	2.55E-07	5.50E-05	2.05E-04	4.33E-05	0.21
37	8.06E-07	9.96E-06	6.83E-04	4.14E-05	4.90E-05	3.31E-04	8.36E-07	9.37E-05	2.08E-04	6.62E-05	0.32
38	1.44E-06	1.03E-04	7.20E-04	1.54E-04	5.17E-05	1.93E-04	3.27E-07	6.91E-05	8.51E-05	7.13E-05	0.84
39	8.39E-07	1.48E-04	6.92E-04	9.71E-05	3.76E-05	2.68E-04	2.18E-07	9.28E-05	1.60E-04	1.11E-04	0.69
40	5.65E-07	8.47E-06	4.69E-04	1.97E-04	2.99E-05	2.06E-04	4.00E-07	9.30E-05	1.37E-04	3.57E-05	0.26
41	4.19E-07	9.89E-06	4.66E-04	2.41E-04	3.60E-05	1.83E-04	4.91E-07	1.26E-04	2.72E-05	7.43E-06	0.27
42	3.71E-07	7.03E-05	8.03E-04	2.64E-05	2.18E-05	1.91E-04	7.64E-07	1.04E-04	6.74E-05	3.33E-05	0.49
43-A1	5.32E-07	8.67E-05	4.12E-04	3.70E-06	1.67E-05	6.31E-05	1.45E-07	2.36E-05	2.76E-05	3.60E-05	1.30
43-A2	1.69E-06	9.47E-05	4.16E-04	3.06E-05	1.77E-05	6.41E-05	1.45E-07	2.33E-05	2.55E-05	2.96E-05	1.16
43-B	5.97E-07	8.51E-05	3.96E-04	3.44E-06	1.53E-05	6.13E-05	1.45E-07	2.11E-05	2.41E-05	2.53E-05	1.05
43-D	7.10E-07	7.92E-05	3.88E-04	3.70E-06	1.78E-05	5.90E-05	1.64E-07	2.13E-05	2.67E-05	2.47E-05	0.93
43-E	7.10E-07	8.04E-05	4.07E-04	3.92E-06	1.77E-05	5.96E-05	9.09E-08	2.30E-05	2.50E-05	2.31E-05	0.92
43-F	9.52E-07	7.88E-05	3.93E-04	3.95E-06	1.64E-05	5.77E-05	1.27E-07	2.10E-05	2.30E-05	2.27E-05	0.99
44	2.05E-06	1.59E-04	6.98E-04	4.24E-05	1.95E-05	1.49E-04	4.00E-07	9.48E-05	6.31E-05	4.93E-05	0.78
45	4.00E-05	5.93E-04	1.45E-03	9.84E-05	5.18E-05	5.66E-04	7.09E-07	4.00E-04	8.28E-05	4.44E-05	0.54
46	6.63E-06	2.84E-05	3.05E-04	8.71E-04	6.00E-06	4.50E-05	9.09E-08	2.37E-05	8.15E-05	2.67E-05	0.33
47	4.71E-05	1.07E-04	1.24E-03	1.66E-04	3.78E-05	3.97E-04	3.09E-07	1.42E-04	1.69E-04	2.00E-05	0.12
48	1.77E-06	7.37E-05	5.50E-04	9.03E-05	2.44E-05	1.82E-04	3.27E-07	7.73E-05	5.92E-05	1.13E-04	1.91